THE ABSORPTION OF SULFUR DIOXIDE BY WATER DROPLETS DURING CONDENSATION

A THESIS

Presented to

The Faculty of the Division of Graduate Studies

by

Thomas Lowell Wills

In Partial Fulfillment

of the Requirements for the Degree

Master of Science in Chemical Engineering

Georgia Institute of Technology

December, 1975

THE ABSORPTION OF SULFUR DIOXIDE BY WATER DROPLETS DURING CONDENSATION

Approved:

Michael J. Matteson, Chairman

William R. Ernst

Jude T. Sommerfeld

Date approved by Chairman: Jan. 13, 1976

ACKNOWLEDGMENTS

In the course of this research, many people have been of assistance and guidance in helping to overcome the unforeseen problems which are a part of any experimental project. In particular, our gratitude is expressed to the following persons:

To Professor Michael Matteson for his guidance in the conceptual design of the experiment and for being a fair and reasonable arbitrator in the face of adversity.

To Phil Shires for help in the design, construction, and troubleshooting of the experimental apparatus.

To John Gay for his invaluable assistance with the instrumentation and for spending many long hours in the laboratory during the experimental runs. It is well that he likes country music.

To Professor Jude T. Sommerfeld for lending his equipment when it was most needed.

To Dave Arnold for helping with the "red tape" during my absence.

And, in particular,

To Mary for her understanding and kindness during the hard times and long hours of loneliness which were involved with this project.

TABLE OF CONTENTS

LIST OF TABLES

LIST OF ILLUSTRATIONS

SUMMARY

Other investigators have shown that the rate of absorption of a gas by a liquid can be accelerated by surface renewal and that current theories do not explain this phenomenon adequately. An experimental study was conducted which measured the rate of absorption of sulfur dioxide by water drops during periods of surface renewal promoted by the condensation of water vapor. The results of this study were compared with the predictions of current theories, and an alternative theory based on surface effects has been postulated.

CHAPTER I

INTRODUCTION

In the past few years pollution has been recognized as being one of our greatest national problems. Ranking in importance just behind the current recession and the continued problem which the energy shortage represents, air pollution constitutes a threat to our quality of life. Although much effort and money are being channeled to end this problem, it continues to grow. In fact, since many solutions which have been proposed for our energy shortage would require an easing of pollution regulations or a return to fossil fuels, the problem of air pollution seems destined to be with us for several years.

Of the various pollutants which constitute the problem of air pollution, sulfur dioxide is released for the most part by stationary coal-burning sources, especially power plants. As part of Project Independence, President Ford has suggested the use of more coal in power plants to reduce our consumption of fuel oil and conserve petroleum. Thus, coupled with an increasing national demand for electricity, the sulfur dioxide air pollution problem is likely to get much worse in the next several years.

The methods currently used to remove sulfur dioxide from stack gases have not yet proven their ability to do the job on full-scale power plants. Previous attempts have been at a reduced scale and have been characterized by low operability and high cost. Thus, more efficient

methods of SO_2 removal from stack gases are needed.

In most of the anti-pollution systems currently in use, wet scrubbing is the mechanism for removing the SO_2. This requires the contacting of the SO_2 laden gases with a liquid (often water) which will absorb the SO_2, effectively removing it from the stack gases. While this principle sounds simple, it has proven to be difficult to accomplish in full-scale applications. Thus, it would be helpful to examine more closely the absorption phenomenon to try to better understand its subtleties and perhaps gain insight which would allow for improved operation of the full-scale units.

This is, however, not an easy task. The system which is being studied is characterized as an unsteady state heterogeneous system of coupled heat and mass transport with a moving interface and complicated flow behavior. Thus, it is not surprising that many of the well-established theories of absorption do not adequately describe this particular system. Specifically, it has been shown by many writers that the penetration and boundary layer theories do not adequately describe systems with continual surface removal.

This phenomenon has been studied experimentally in the past by measuring the mass transport during drop formation in liquid-liquid and gas-liquid systems, and by measuring the effect of a surface electrical charge on absorption. In each case it has been found that (1) the transport is greater than during steady state absorption and (2) the theories proposed for transient absorption are not adequate to describe the nature of this process quantitatively.

It is with this background that a program was undertaken to design

an experimental apparatus and test these theories during another type of surface disturbance--that of surface replacement during condensation.

This particular system was chosen due to evidence that surface effects ignored by all other theories may be the dominant factors in controlling unsteady interphase mass transport. In addition, this type of system closely approximates the natural condensation process which occurs in clouds and during the condensation of humid smoke stack plumes. Thus, an explanation for the surprisingly low values of ground level SO_2 from smoke stack discharges could be found in the absorption of high amounts of this gas as the warm humid gases condense upon exiting the stack. Also, it may be possible to explain the surprisingly high amounts of sulfate (and nitrate) found in clouds by the same mechanism. Finally, the synergistic action of SO_2 with soot (condensation nuclei) to cause great breathing problems could be given further explanation.

CHAPTER II

THEORETICAL DEVELOPMENT

The absorption of one component of a gas mixture by a liquid droplet during drop formation, release, acceleration, and fall with condensation of the liquid vapor is an extremely complex process. The basic process can be characterized as an unsteady state system of interphase multicomponent mass transport with coupled heat transport. One must also consider the fluid mechanics, liquid phase chemical reaction, and surface effects involved.

Even in the absence of condensation, the theoretical description of such a process has been very difficult, with the results of the various theories differing greatly based on the assumptions which were chosen. In their discussion of interphase mass transport, Bird, Stewart, and Lightfoot (6) point out some of the problems associated with this type of system,

> Two-fluid mass-transfer systems offer many challenging problems: The flow behavior is complicated, the moving interface is virtually inaccessible to sampling, the interfacial area is usually unknown, and many of the practically important systems involve liquid phase chemical reactions. A better basic understanding of these systems is needed.

Historically, the absorption of a gas by a liquid has been described by three theories: film theory, boundary layer theory, and penetration theory. Each views the problem in a different light, involves different assumptions, and thus arrives at different conclusions.

The film theory was the earliest attempt to define absorption and is characterized by the gross assumption of steady state. This theory would more correctly be called the two-resistance theory, for it visualizes a stagnant film in each phase which constitutes the resistance to mass transfer. One defines an effective film thickness, X_L, as the depth of film over which the concentration varies. Additional assumptions are:

1. Complete mixing in both bulk phases.

2. Chemical equilibrium at the interface (Henry's law) and no resistance to transfer at the interface.

If, in addition, one assumes that the liquid film resistance is the more dominant, one arrives at the following equation for the rate of absorption:

$$N_A = \frac{D_{AB}(C_{AS} - C_{A\infty})}{X_L} = K_C(C_{AS} - C_{A\infty}) \qquad (1)$$

This theory has been the basis for the classical explanation of the phenomena of gas absorption and is still taught today. However, there are several difficulties with this theory. As pointed out by Danckwerts (12), this theory presents an unrealistic picture of the absorption mechanism. Danckwerts abandoned the usual assumption of a stagnant film at the interface and suggested that a better model was one in which the surface is continually replaced with fresh liquid. He maintained that the gas and liquid do not attain immediate equilibrium at the interface.

In 1935 Higbie (28) proposed the penetration theory based on the rationale that steady state is never reached in industrial mass transfer equipment, and the transfer process is controlled by what happens in the

liquid film during the penetration period.

The basic equation for describing the absorption process is Fick's Second Law:

$$\frac{dC_A}{dt} = D_{AB} \frac{d^2C_A}{dX^2} \tag{2}$$

with boundary conditions:

at $t = 0$ $\quad C_A = C_{AO}$

at $X = 0$ $\quad C_A = C_{AS}$

at $X \rightarrow \infty$ $\quad C_A = C_{AO}$

The solution of this equation describes the rate of absorption as a function of time (24).

$$N_A = (C_{AS} - C_{AO}) \sqrt{\frac{D_{AB}}{\pi t}} = K_C (C_{AS} - C_{AO}) \tag{3}$$

Comparison of this equation with Equation 1 shows that the penetration theory predicts that the mass transfer coefficient, K_C, varies inversely with the square root of time and would be very large at small exposure times.

Higbie (28) found that this theory somewhat overestimates the rate of transport at short exposure times and postulated,

> The progressively greater deviation from the penetration theory with shorter periods of exposure seems to indicate an additional resistance to absorption which is especially effective for shorter periods. This may very well be an extra resistance of some kind at the surface.

The penetration theory is particularly well suited to interfaces which are not stationary, for example, a falling liquid film in the pres-

ence of a gas, when there is a flat velocity profile near the interface.

The more recent boundary layer theory differs from the film and penetration theories in that allowance is made for two-dimensional velocity profiles at the interface. In this approach, the mass transport phenomena are assumed to be analogous to heat transfer phenomena with the resulting equation relating dimensionless groups.

$$Sh = 2.0 + 0.6\ Re^{1/2}\ Sc^{1/3} \tag{4}$$

However, Angelo (2) has shown that during continual periods of surface renewal, the actual mass transfer coefficient may be as much as 15 times as large as that predicted by boundary layer calculations alone. Moreover, Ward (57) has concluded that this approach should not be applicable to the case of a droplet absorbing a gas.

The main conclusion that can be drawn from the three principal theories of mass transfer is that they are inadequate for describing the unsteady state absorption of gases by spheres in condensing systems. A review of the literature shows that there is a great gap between theory and experiment.

Most of the recent experimental work has involved studies of the droplet formation period wherein the droplet is growing by issuing from a capillary tip. This mechanism may be useful in characterizing sprays or jets, but it does not adequately describe fog or cloud formation. Angelo (2) developed the surface stretch model of surface renewal. Groothius and Kramers (24) and later Beek and Kramers (4) developed a model which predicts mass transfer coefficients based on the continuous forma-

tion of fresh surface during droplet growth. Rajan and Heideger (45) have shown that internal circulation is a critical parameter and that Kramers' theory does not correlate well with the work of other investigators. Dixon and Russell (15) observed very high absorption rates during drop formation, which they concluded were due to turbulence within the droplet.

It is, therefore, necessary to separate studies which incorporate internal droplet mixing as a mechanism in the mass transfer to a growing droplet from those where mass transfer is to a droplet growing by condensation with no internal turbulence in the liquid core. Bogaevskii (7) has reported on such a situation. Upon observing the condensation of humid SO_2-laden vapors in a mine shaft, he has reported that these water droplets growing by vapor condensation absorb 5.7 to 7.2 times more SO_2 than predicted by steady state absorption considerations. Moreover, this resulted in a supersaturated solution of SO_2 in the liquid phase which required as much as one hour before the excess SO_2 was liberated and the equilibrium concentration was reached. Clearly, the assumption of equilibrium (Henry's Law) at the interface must be seriously questioned.

In work recently completed (14,22,40), attention has been focused on certain surface characteristics of water. It has been known for some time that very dilute solutions of water (10^{-3} to 10^{-5} N) exhibit certain anomalities with regard to viscosity and surface tension. Jones and Ray (32) have shown that the surface tension of dilute salt solutions actually declines with increasing concentration, passing through a minimum at 2.0×10^{-3} N and then beginning to increase according to predictions based on the Onsager-Samaras theory. This initial decrease may indicate an adsorp-

tion of ions at the surface. It would appear that this adsorption continues until a specific number of sites is occupied; further increases in ionic concentration result in their rejection from the surface. A simple calculation reveals that the concentration of these sites at the interface surface (based on the minima at 2.0×10^{-3} N) is four sites per 10^5 water molecules. It is hypothesized that these sites play a significant role in the absorption of a gas by water.

In recent experiments (22), this assumption was tested by the application of an electrical charge to the surface of a water droplet, and for increasing surface charge densities the rates of SO_2 absorption were compared to those without charge. The number density of surface molecules was then increased by the exertion of a surface pressure. A slope-intercept technique was used to estimate the number density of surface receptors (or sites) at zero applied charge. This value was found to be 4.2 sites per 10^5 surface molecules, much in agreement with the values obtained from Jones-Ray measurements. In addition, the depth of the equilibrium air-water surface electrical double layer was estimated to be between 0.3 and 3.0 μm.

The significance of these results is that, in the case of aerosols, where the liquid phase is usually present in droplets smaller than five μm in diameter and with the majority of droplets lying in the submicron range, ordinary bulk phase mass transfer mechanisms do not apply.

Very little is known about the chemical nature of the air-water interface. However, from the above results, it seems reasonable to conclude that the uptake of foreign gases by micron-sized water droplets is primarily a surface phenomenon. Moreover, surface sites function much

like those found in gas-solid adsorption where there is a selectivity which determines how much of each species will be adsorbed and what particular surface concentration will be maintained. Most significant in terms of gas entrapment by aerosols would be the case of trace gases (such as SO_2) which are encountered in air pollution situations.

The exact nature of these receptor molecules, or sites, is not clear. However, Drost-Hansen (16) has characterized them as cage-like water polymers carrying a hydroxyl ion and oriented in fixed fashion so as to make up the upper, ordered component of the electrical double layer.

We have speculated on the mechanism by which these site molecules participate in the absorption process. Of the many gas molecules which strike the surface a few remain attached. These migrate to a site molecule and become either complexed chemically or hydrolyzed and then bound to the structured water polymer. It is then necessary for the attached group to diffuse out of the surface zone and into the bulk of the solution. In the case of normal steady-state absorption, this latter step is rate controlling, and it is this process which dominates the mass transfer operation. However, in the case of aerosols, where the bulk liquid does not extend past the surface double layer thickness, the adsorption mechanism is more likely to predominate.

Naturally as the sites become saturated in the case of the aerosol, the transfer would cease. But if water vapor is continually condensed on the aerosol surface, new surface is being created and new sites are formed at a rate determined by the rate of condensation. We might expect, then, that the unsteady-state condensation mechanism not only increases the rate of mass transfer, but also tends to supersaturate the growing droplets

with respect to SO_2. Once the growth stops, there would have to be a desorption of SO_2 until the equilibrium saturation concentration is reached in the bulk liquid phase. However, in most condensation nuclei there exist soluble ions such as Mg^{++} or NH_4^+. These ions act to complex with and trap the dissolved SO_2 (as HSC_3^- ions) and thus allow less SO_2 to escape.

In order to experimentally test for this surface phenomenon, it is necessary to design an experiment where the effects of drop formation, internal drop turbulence, and acceleration can be separated from those affecting the adsorption process. What is proposed is to measure mass transfer rates in the absence of water vapor. The internal turbulence in the droplet is at a minimum after the droplet has detached from the capillary and is in free fall. To identify the effects of drop formation on mass transfer, the falling distance is varied and the rate of mass transfer measured versus distance (or falling time). When the falling distance is extrapolated to zero, one can determine the SO_2 absorbed during drop formation.

The next step is to repeat this procedure in the presence of a humid air-SO_2 mixture. The information desired is the influence of the rate of condensation on the rate of SO_2 absorbed by the droplet. The droplets are collected in a tube separated from the main SO_2 atmosphere by an inert sheath. The tube contains a solution of H_2O_2, which rapidly oxidizes the SO_2 in the droplets to prevent desorption. The solution is then analyzed for pH to determine the amount of SO_2 collected.

This procedure allows one to subtract both the drop formation period and free fall turbulence effects in assessing the mechanism of

condensation in the mass transfer of SO_2 to a droplet. The advantages in using a single droplet technique are that the sizes can be controlled and measured, and it is easier to control the temperature in such a system.

In order to evaluate the effect of condensation on the adsorption rate, it is necessary to know the rate of growth of surface area due to condensation. It has been shown (19,27) that this relationship is,

$$S_o - S = \frac{\rho_{AS}\ 8\pi D_{AB}}{\rho_L}\left(\frac{\rho_{A\infty}}{\rho_{AS}} - 1\right)t \tag{5}$$

where $\frac{\rho_{A\infty}}{\rho_{AS}}$ is the supersaturation ratio, SSR.
Thus, one would expect the surface renewal due to condensation to be proportional to the supersaturation ratio.

Another possible effect which could influence the rate of adsorption is Stephan Flow. This is the physical trapping of SO_2 molecules into the liquid phase due to their being swept along by the condensing water vapor. This would be analogous to going the wrong way on a one-way street during rush hour. The relationship (18) for calculating the effect of Stephan Flow is

$$R_{SF} = \frac{D_{AB}P}{RT} \ln\left[\frac{P - P_{sat}}{P - P_{o1}}\right] \tag{6}$$

It is also possible to calculate the rate at which molecules of SO_2 would strike the surface of the water droplet due to their random kinetic motion. This relationship is

$$R_{kE} = \frac{P}{\sqrt{2\pi\ RTM_A}} \tag{7}$$

Finally a method is needed to predict the effect of condensation on the absorption of sulfur dioxide. If one assumes that the flux of SO_2 is proportional to the flux due to condensation, then

$$\frac{dN_{SO_2}}{dt} = KY_{SO_2} N_{SO_2} \frac{dN_{H_2O}}{dt} \tag{8}$$

which has the solution upon integrating

$$\ln \frac{N_{SO_2}}{(N_{SO_2})_o} = KY_{SO_2} N_{H_2O} \tag{9}$$

This theory would predict that the rate of absorption is dependent on the rate of surface renewal due to condensation. A semilog plot of SO_2 absorption versus condensation should give a straight line at a specified gas phase SO_2 concentration.

The ability of condensing water to absorb more SO_2 than predicted by equilibrium considerations is in part due to the extremely fast hydrolysis reaction undergone by SO_2 in water,

$$SO_2 + H_2O \underset{k_2}{\overset{k_1}{\rightleftharpoons}} HSO_3^- + H^+$$

where

$$k_1 = 3.4 \times 10^6 \text{ sec}^{-1}$$

$$k_2 = 2.0 \times 10^8 \left(\frac{\text{gmol}}{\ell}\right)^{-1} \text{ sec}^{-1}$$

This is one of the fastest hydrolysis reactions known which will temporarily "trap" the SO_2 in the liquid phase.

CHAPTER III

INSTRUMENTATION AND EQUIPMENT

While the various gas and liquid handling systems with their endlessly winding labyrinth of tubing and wire and valves and meters attracted one's initial attention, the heart of the experimental apparatus was the glass contacting chamber with variable length vertical sections. This is shown schematically in Figure 1. This contacting chamber was hand blown in the Georgia Tech Glass Blowing Laboratory and consists of the baffled mixing chamber, the contacting chamber, several straight sections used to vary the vertical distance, and a gas-sheathing and droplet collecting chamber. Several drains served to remove condensate and were connected to the drain system.

The top of the contacting chamber was a large rubber stopper with a silicone grease seal. Holes were drilled through this stopper to allow the hypodermic needle, thermometer, and gas sampling tubes to penetrate into the contacting chamber. The needle was a 24-gauge hypodermic needle with the end squared off and polished. A picture of a drop perched on the needle end showed that the drops were spherical in shape.

The baffled mixing tube was sealed on the exterior by cementing on a plexiglass plate. The gases were delivered into the chamber by tubing ended in Swagelok fittings which were screwed into the plexiglass plate.

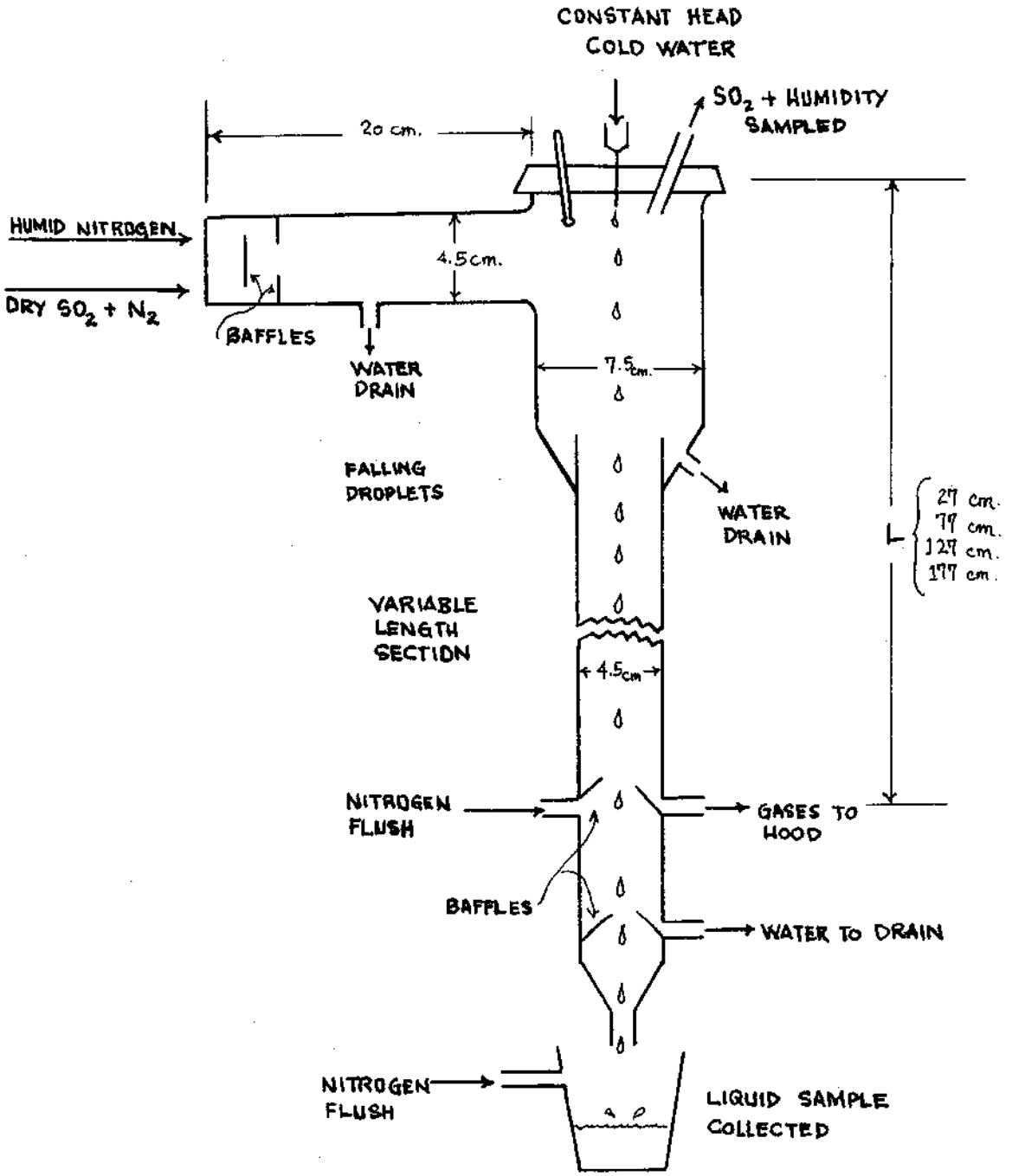

Figure 1. Schematic Diagram of Contacting Chamber

The sheath section was a complex double compartment glass chamber which featured two 1.5 cm holes through which the droplets deftly passed before being collected in a test tube. The second chamber and test tube were sheathed in nitrogen to prevent unsteady absorption as the droplets broke up. This section connected to the variable length vertical tubes, which connect to the contacting chamber with ground glass fittings.

This entire glass system was supported from a temporary laboratory rack (3 x 1.5 m) by numerous clamps. Initially, the entire glass system was wrapped with heater tape and insulated, but this was found to be unnecessary and was removed. The supporting rack and all electronics were well grounded.

In order to be able to accurately control the various parameters, an experimental apparatus was constructed which incorporated several systems into one unit. It was, in general, necessary to perform the following functions: the gases had to be precisely metered, mixed, and humidified before delivery into the contacting chamber; the water had to be cooled, purified, and delivered at constant flow rate to the needle inside the contacting chamber; the gas composition, humidity, and temperature had to be monitored; the liquid had to be collected for analysis after contacting; and it was necessary to maintain a nitrogen flush system, a system for gas removal to the hood, and a sump system for condensate drainage. The various components of the apparatus will be considered in groups according to their function.

The gas delivery system is shown schematically in Figure 2. The purpose of this system is to quantitatively combine the nitrogen, sulfur dioxide, and water vapor in such a manner that the concentration of SO_2

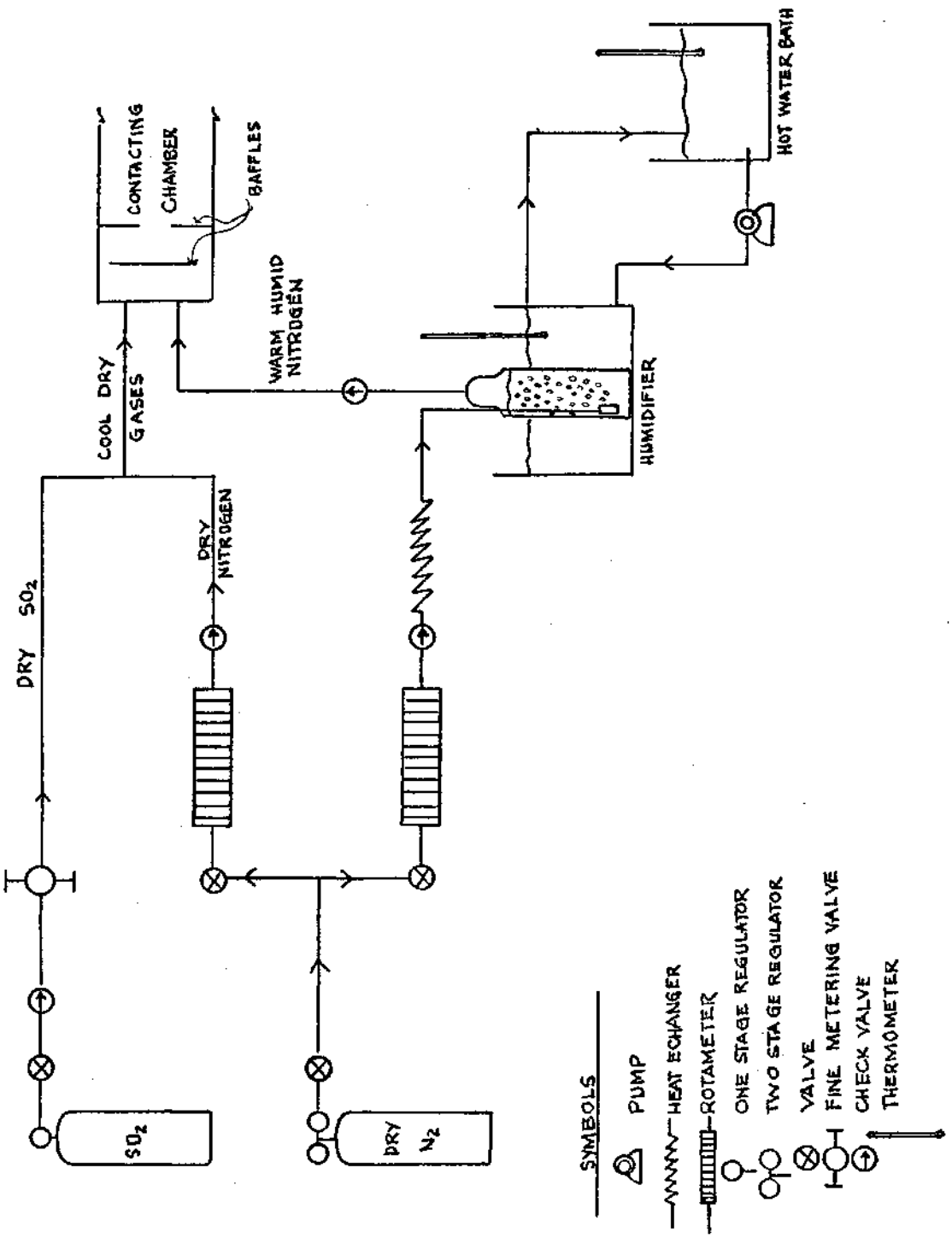

Figure 2. Schematic Diagram of Gas Delivery System

in the mixture could be controlled within five percent and that the supersaturation ratio could be controlled within 10 percent.

The gases were delivered to the contacting chamber in two streams, one warm and humid, the other cool and dry. The warm gas stream consisted of humid nitrogen with no SO_2. This was controlled by bleeding high purity oxygen-free nitrogen from a cylinder through a needle valve, a rotameter, a check valve, a heat exchange coil, a humidifier which was maintained at an elevated temperature by external circulation of warm water from a Haake Model FK2 Constant Temperature Bath, a check valve, and finally into the contacting chamber. The cool, dry gases were composed of nitrogen and sulfur dioxide. The sulfur dioxide was bled from a cylinder through a needle valve, a check valve, a precise micro-metering valve, and combined with the nitrogen in a tee. The nitrogen came from the same cylinder as the humid nitrogen and was passed through a needle valve, a rotameter, and a check valve before combining with the SO_2 and introduction into the contacting chamber.

The gas sampling system is shown schematically in Figure 3. The purpose of this system is to take samples of the gases in the contacting chamber which are representative of the conditions existing near the falling water droplets. This is accomplished by continuously removing gas from the contacting chamber at a point approximately one centimeter below and one centimeter offset from the hypodermic needle. Thus, the samples taken were representative of the conditions near the forming droplet. These conditions were shown to prevail throughout the length of the vertical tubes as no change in composition could be detected.

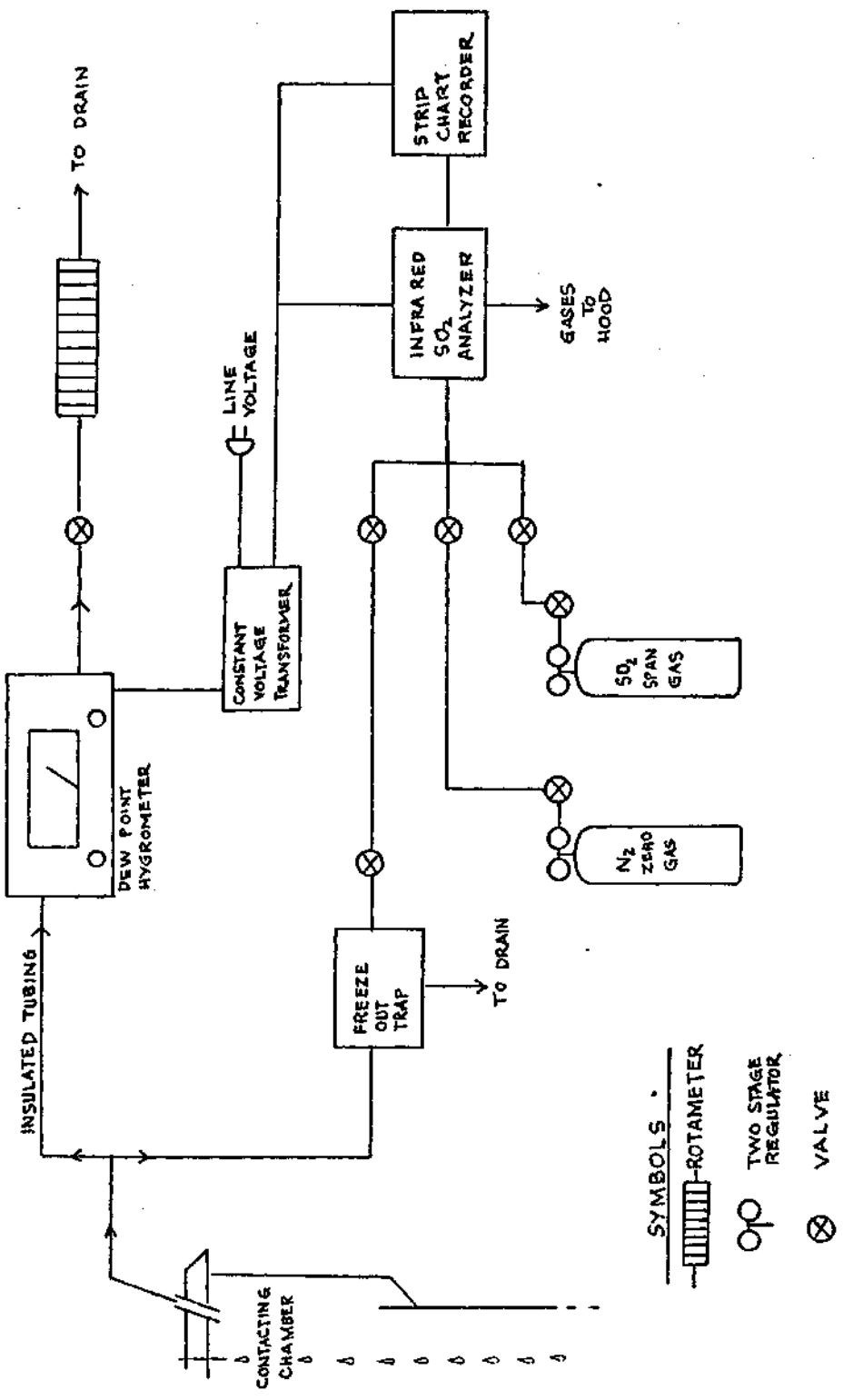

Figure 3. Schematic Diagram of Gas Sampling System

These gases were split to be sent to the humidity analyzer and the SO_2 analyzer. Gases were drawn by a partial vacuum through insulated tubing (to minimize condensation and heat transfer) into a Cambridge Systems Model 880 Thermoelectric Dew Point Hygrometer followed by a needle valve and a rotameter. Samples were analyzed periodically for dew point in the absence of SO_2 in order to protect this meter. The second gas stream was drawn by a partial vacuum through a freeze-out trap maintained at -12°C to keep the humidity constant in order to remove interference in the infrared SO_2 analysis. The gases were analyzed with a Beckman Model 215A Infrared Sulfur Dioxide Analyzer equipped with a Coleman-Hitachi Model 165 Strip Chart Recorder. The hygrometer, SO_2 analyzer, and recorder were connected to a constant voltage transformer to reduce errors caused by fluctuations in line voltage.

After contacting, the falling droplets were collected in a test tube held below the gas sheath chamber. Both the test tube and the sheath chamber were blanketed by nitrogen to eliminate absorption when the falling drops hit either the funnel or test tube wall. The gases and any condensed humidity were removed to the hood and drain by the vacuum system. After collection, the liquid was analyzed for acidity with a Beckman Zeromatic pH Meter.

The vacuum system served to remove toxic gases to the hood, condensed water to the drain, and provided a means to draw gaseous samples through the sampling system. This system was comprised of three aspirators, two connected to a vacuum flask and the third to a plexiglass tank. The aspirators were run continuously. Into these vacuum vessels, tubes

ran which connected to all drain and flush points. These were valved by screw clamps or pinch cocks to provide a small bleed or an intermittent drain as the need dictated. At the flush points, gas was continuously bled to the aspirator to the hood.

The final system, the water supply system, served to supply high purity water at a constant flow rate and temperature to the hypodermic needle. Distilled, deionized water with a resistance greater than 1.5×10^5 ohms was stored in a 20-liter carboy under a nitrogen blanket. This water flowed by gravity into an ion exchange medium which removed dissolved oxygen, cations, and anions. It was then pumped to a tank which provided a constant head to the needle. This tank had an inlet, outlet, and a larger diameter standpipe to maintain a constant liquid height in the tank. The pumping rate was set to maintain a continuous trickle of water coming out of the standpipe to the drain. The constant head tank was covered and blanketed in nitrogen. From this tank the water flowed by gravity through a countercurrent heat exchanger and into the needle. The heat exchanger circulated a glycerol-water (50 percent) mixture which was maintained precisely at -12°C by a Precision Scientific Lo/Temptrol Constant Temperature Bath. The water had a residence time of approximately one hour in the heat exchanger and left the hypodermic needle as droplets at 7°C.

This completes the description of the experimental apparatus.

CHAPTER IV

PROCEDURE AND DATA ANALYSIS

The functions of this chapter are, first, to describe the procedure used in making an experimental run in sufficient detail to allow a technically competent person to go into the laboratory and conduct a typical run and, second, to illustrate the analysis of the experimental data and make an estimate of the error involved in the data and in the calculations made using the data.

Prior to making an experimental run, several preparations were required. First, the strip chart recorder, hygrometer, and pH meter were connected to the constant voltage transformer and allowed to warm up for a minimum period of 30 minutes. The hot water bath was turned on, and the water temperature allowed to equilibrate. (The cold water bath was continuously in service due to the six-hour period required for equilibration from room temperature.) The infrared analyzer, which would normally require a significant warmup, was kept "hot" so that it needed no warmup. While the other instruments were being warmed, the infrared analyzer was calibrated. To calibrate the analyzer, the zero gas, dry nitrogen, was passed through the instrument and the output set to zero. Next a span gas of known sulfur dioxide concentration was passed through the instrument and the gain was adjusted to give the reading that corresponded to the factory calibration curve for the known concentration. Then, dry nitrogen was connected to the analyzer, and the zero point

rechecked. The strip chart recorder was calibrated simultaneously with the analyzer.

During the preparatory period, the pump for the droplet water was turned on and a steady flow was established from the constant head chamber through the heat exchanger and finally to the needle. The drop rate, flow rate, and temperature were checked after the system had come to steady state. The pH meter was calibrated with a standard buffer solution and checked with a second buffer solution.

The aspirators and hood were commissioned to establish the drain and vacuum systems and the apparatus was purged with dry nitrogen. The sheath nitrogen streams were started, and the humidity was adjusted with the warm nitrogen to give the desired wet bulb temperature. Next the sulfur dioxide was metered into the gas stream until the concentration required for this run was attained. After allowing a few minutes for stabilization, sampling was begun.

At this point a run was in progress. Readings of the dew point hygrometer, the strip chart recorder, the dry bulb temperature of the gas streams, the temperature of the droplet water, and the temperature of the circulating water baths were monitored. These values were controlled throughout the run for constancy. The variable length sections which are attached to the contacting chamber and the collection chamber (at the bottom) were checked for condensed humidity and drained if necessary. After allowing a few moments to assure steady conditions, a test tube was connected to the bottom of the collection chamber and flushed with nitrogen. The temperature of the collecting liquid was measured, and the system finally checked to be sure there was a slight positive pressure so

that no room air would dilute the contacting gases.

Following this last check, the five ml of the solution collected in a fresh sampling tube were transferred to another tube and rapidly mixed with one ml of a three percent hydrogen peroxide solution. This oxidized the absorbed SO_2 to the sulfate state and effectively "fixed" the concentration of the solution. After allowing a few minutes for the solution to reach thermal equilibrium at room temperature, the pH was analyzed, thus determining the sulfate concentration. At each length-humidity-concentration combination, at least two samples were taken and analyzed. During the initial phase of the sampling program, tests were conducted in triplicate. However, early results indicated that two trials would be sufficient. So, in the interest of time saving, the duplicate procedure was adopted.

One particular set of data was collected at a specified supersaturation ratio, since this took longer to change than either the SO_2 concentration or the exposure length, and also was stable and needed little attention. Therefore, at one supersaturation ratio, data were taken at one SO_2 concentration for four exposure lengths. Changing the length was sometimes uncomfortable at high SO_2 concentrations, and the air in the laboratory room was continuously circulated by a fan. After sampling at the four lengths, the SO_2 concentration was increased to the next level and the process repeated. Approximately six hours were required at each supersaturation ratio for a complete set of uninterrupted sampling by two experimenters.

Attention can now be turned to the second function of this chapter, the data analysis. Any errors in the data analysis are either sampling

and measurment errors or systematic errors. The latter type would include those arising from the lack of control of a system parameter or a failure of the validity of one of the assumptions concerning the contacting conditions.

In order to minimize errors in measurement, the instruments were checked against accurate standards. The infrared analyzer, the strip chart recorder, the dew point hygrometer, and the pH meter were calibrated before use. The rotameters in the air flow were calibrated by measuring a volume of gas which passed at a constant rate by water displacement. The factory curves were found to be adequate.

In each experiment, a number of assumptions was made about the validity of the measurements and the experimental conditions. It was assumed that the gases were well mixed, and no gradients of SO_2 concentration, temperature, or humidity existed within the contact chamber or through the variable length sections to the collection chamber. This assumption was checked several times, and no gradients were detected.

Even though this process of mass transport is obviously a coupled system of simultaneous heat and mass transport, it is assumed that heat transfer effects are small and can be neglected. In order to justify this assumption the heat transfer coefficient, h, was estimated by

$$Nu = \frac{hD_p}{K} = 2.0 + 0.6\ Re^{1/2}\ Pr^{1/3} \tag{10}$$

Then the total heat transferred to the drop by convection and condensation is

$$Q = mC_p\Delta T = [hS(T_{N_2} - T_D) + W\lambda]texp \tag{11}$$

where W is the mass of water condensed per unit time calculated from

$$W = K_X S(\bar{P}_W - P_{OW})/P \tag{12}$$

and K_X is the mass transfer coefficient, calculated by

$$Sh = \left[\frac{K_X D_P}{C D_{HW}}\right]_{film} = 2.0 + 0.6 \, Re^{1/2} \, Sc^{1/3} \tag{13}$$

These calculations indicate that the expected rise in droplet temperature is about 1.0°C. Experimentally, an attempt was made to check the temperature of the droplet upon collection. An approximate change of temperature from 7°C at the needle tip to 9°C at the sample collector point was observed. Therefore, based both on theoretical predictions and some experimental data, the assumption that the heat effects are small is valid, and this system will be treated as an isothermal one with average physical properties being used.

It was assumed that the properties of the droplet water remained constant throughout the experiment; that is, the drop rate, flow rate, temperature, and purity remained constant. Checks of these indicated that this assumption was justified.

It was also assumed that no sulfur dioxide was absorbed after the drops were inside the collection chamber. In order to ensure this, the nitrogen sheath was maintained at a significantly high flow rate to keep the chamber and collection tube in an inert atmosphere. Further, it was assumed that no significant desorption occurred as the droplet struck the funnel or while it waited in the sample tube before being fixed with the

peroxide. In order to test the latter assumption, a simple test was made to try to observe a decrease in the dissolved SO_2 concentration as a function of time. It was observed that for a very few minutes the dissolved SO_2 concentration remained the same; but as the solution temperature increased, the concentration decreased. It was, thus, necessary to "fix" the solution with peroxide as soon as possible after taking the sample.

In order to establish a base point from which to compare other data, samples were collected with no SO_2 present in the contacting chamber and no observable level of sulfate was found after fixation with peroxide. This reduces the possible concern about interference from other gases being absorbed and measured by the nonspecific pH method. In addition, samples were taken for each sulfur dioxide concentration at a supersaturation ratio equal to 1.0 (no condensation). Thus, the effects of increasing the rate of condensation upon absorption could be monitored.

This concludes the description of the procedure used in making experimental runs. Following this procedure, 23 runs were conducted using sulfur dioxide as the absorbate and another 17 with oxygen. These raw data are summarized in Appendix B.

Next, the manner in which the data were used to calculate the quantities of interest will be reviewed.

The drop rate, DR in drops/minute, was calculated by manually counting the number of drops falling in a period of time. Simultaneously, the drops were collected so that the volumetric flow rate, $\dot{V}$, in cm^3/min, was also determined. Thus, the volume per drop, V, was calculated from:

$$V = \dot{V}/DR \qquad (14)$$

From this volume, the radius per drop was calculated by:

$$r_p = \left(\frac{3V}{4\pi}\right)^{1/3} \tag{15}$$

In order to determine the exposure time for a given column length, the terminal velocity of the droplet was calculated. This was done by assuming that the droplet was falling in the Newton's Law flow regime, or:

$$\frac{d\nu}{dt} = g(1 - C^2\nu^2) \tag{16}$$

where

$$C^2 = \frac{1/2\ \rho_{N_2}\pi\ r_P^2 C_D}{4/3\ \pi r_P^3\ \rho_P g} \tag{17}$$

and C_D is the drag coefficient. By assuming a constant C_D and integrating,

$$\nu = \nu_t \tanh\ (cgt) \tag{18}$$

By integrating once more, one gets the exposure time corresponding to a given distance

$$t_{exp} = \frac{1}{cg}\ \text{Cosh}^{-1}\ (c^2 gx) \tag{19}$$

Therefore, a trial-and-error procedure is used to calculate the exposure time. First an estimate of the velocity is made, then the Reynolds number,

$$R_e = \frac{\rho_{N_2} V_P \nu}{\mu_{N_2}} \tag{20}$$

is calculated using properties of water at 8°C. Next the drag coefficient is determined and finally the velocity and exposure time calculated. This procedure is repeated until the velocities agree.

Finally, the concentration of absorbed SO_2 was calculated as fixed sulfate, SO_4, from the pH. The calibration curve shown in Figure 4 was used in this calculation.

The accuracy and precision of these calculations are difficult to estimate. The temperature of the droplet was accurate within two degrees. This could cause small errors in determination of terminal velocity and larger errors in diffusivity, viscosity, and Henry's law constant.

The liquid phase SO_4 concentration could be measured within five percent. The gas phase SO_2 analysis is also within five percent error. The supersaturation ratio calculated via the wet and dry bulb temperature is subject to up to 10 percent error due to marginal controlability of these temperatures. While the wet and dry bulb temperatures were very stable over a fairly long period of time, they were subject to some short term variation due to air currents and surges of humid air in the gas delivery system.

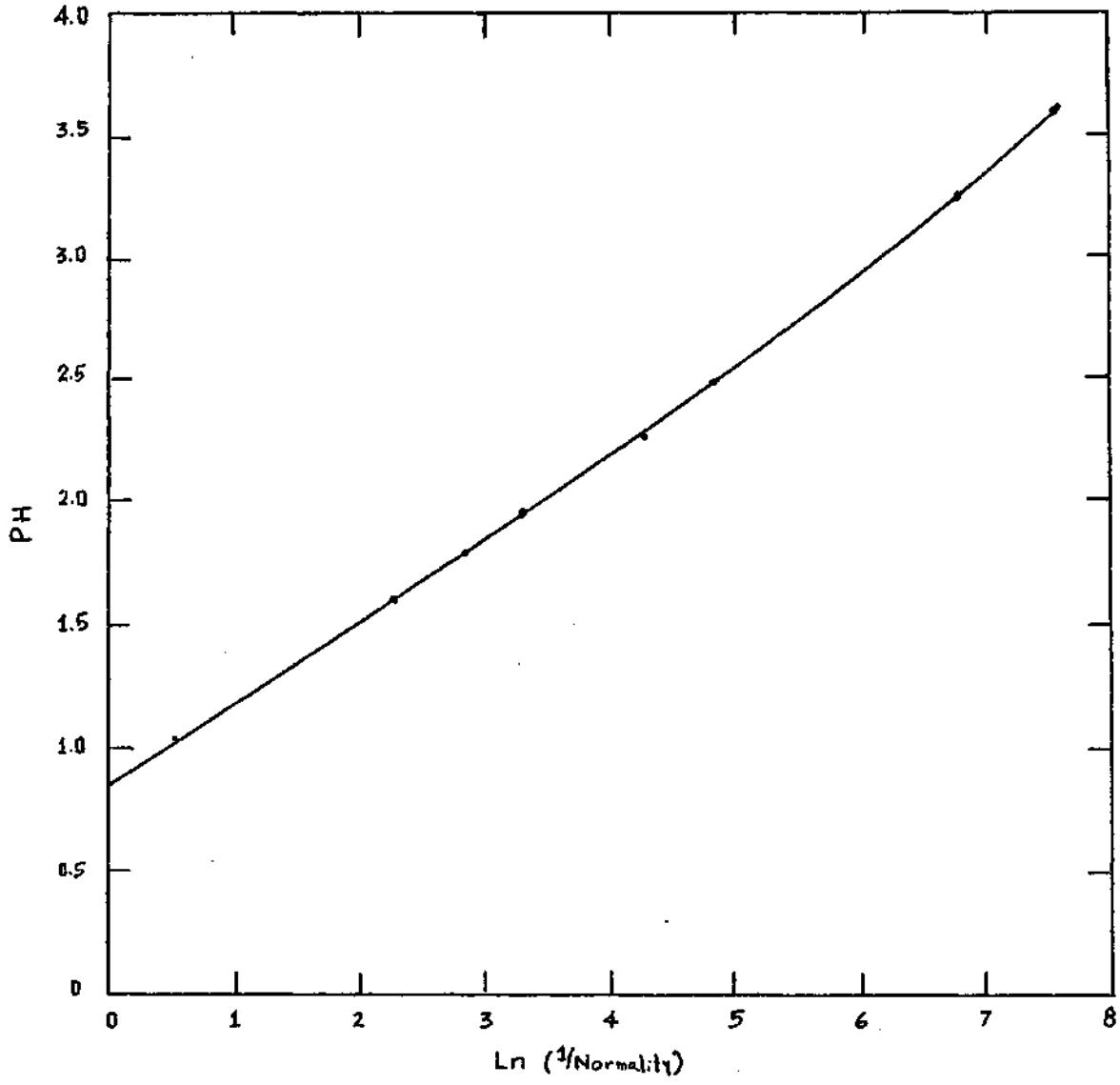

Ln (1/N) versus PH

Figure 4. SO_4 Calibration Curve

CHAPTER V

DISCUSSION OF RESULTS

The measured parameters for all runs are listed in Appendix C. Graphic presentation of these results is incorporated into this chapter.

Before describing the individual graphs, however, some general remarks about the data are in order. First, at the time of absorption, slight temperature changes occurred in the droplets due to the absorption. No effort was made to take these effects into account. Accurately quantifying such temperature changes was thought to be too difficult to do experimentally, and, also, it was thought that these effects would be inconsequential in comparison with other phenomena that were occurring. Second, flow rates were kept constant throughout the course of any given run, but there was slight run-to-run variation in the water flow rate through the capillary. Due to the small magnitude of this drift, which was of the order of one percent, no special accounting of this change was attempted. Third, Schroetter (49) and other investigators have verified that the presence of surface agents may cause a reduction in the rate of sulfur dioxide absorption. Although distilled, de-ionized water was used exclusively in the experimentation, it was not known if any corrosion products had entered the water stream from the stainless steel hypodermic needle. This error was assumed to be small since the needle was cleaned prior to each series of run.

Upon examining the data taken when analyzing for the absorption of oxygen, it rapidly becomes obvious that the analysis is not correct. Many of the data points would indicate a negative concentration of oxygen in the collected droplets; several more would indicate concentrations far in excess of the equilibrium saturation concentrations at the experimental temperature. Even tests which were designed to look for the concentrations of oxygen in a saturated water sample yielded results which were impossible to explain. The most probable explanation for this result would be the improper use of the Natelson Microgas Analyzer which was used to analyze the dissolved oxygen in the water. With this complete lack of precision in the oxygen data, it was decided that no analysis would be conducted with it, and it was not considered further.

The sulfur dioxide data consist of 23 runs (or cases) totaling 179 data points. Of these, two were blanks with no sulfur dioxide and 15 were unreliable due to problems noted at the time of taking the data. This leaves 162 data points which constitute the data base for this analysis.

In order to obtain a general feeling for the relationship of the absorbed sulfate as a function of sulfur dioxide concentration, supersaturation ratio, and exposure time, a stepwise multiple regression analysis was conducted using the modified (162 points) data base. This showed that the gas phase sulfur dioxide concentration is the most significant variable and that exposure time is the least significant. Table 1 summarizes this analysis.

Table 1. Multiple Regression Analysis of the Modified Data Base

Variable	Correlation Coefficient	T-Value
SO_2	0.66	16.7
SSR	0.32	10.4
T_{exp}	0.27	6.3

In order to measure the effect of the carrier gas on the results, experiments were conducted at an SSR = 2 and a SO_2 = 2000 ppm. Run 11 is identical to Run 12 except that dry nitrogen was used as the carrier gas in the former and dry air in the latter. There was no significant difference between the results of these two runs. Figure 5 shows the effect of exposure time on SO_2 absorption for Runs 11 and 12.

Equation 3, which represents the solution to Fick's Second Law based on the assumptions of the Penetration Theory, predicts that in the absence of condensation the flux of SO_2 absorbed will be proportional to the gas phase SO_2 concentration divided by $t_{exp}^{1/2}$. Figure 6 shows the data for SSR = 1 plotted in this fashion. While there is some scatter, the data support the Penetration Theory for a non-condensing system.

Figures 7 and 8 show the effect of SSR and SO_2, respectively, on the moles of SO_2 absorbed during condensation. Figure 7 clearly shows that at a constant gas phase SO_2 level (3000 ppm), the moles of SO_2 absorbed is a linear function of time and increases with supersaturation ratio. Similarly, Figure 8 shows the effect of gas phase SO_2 concentration

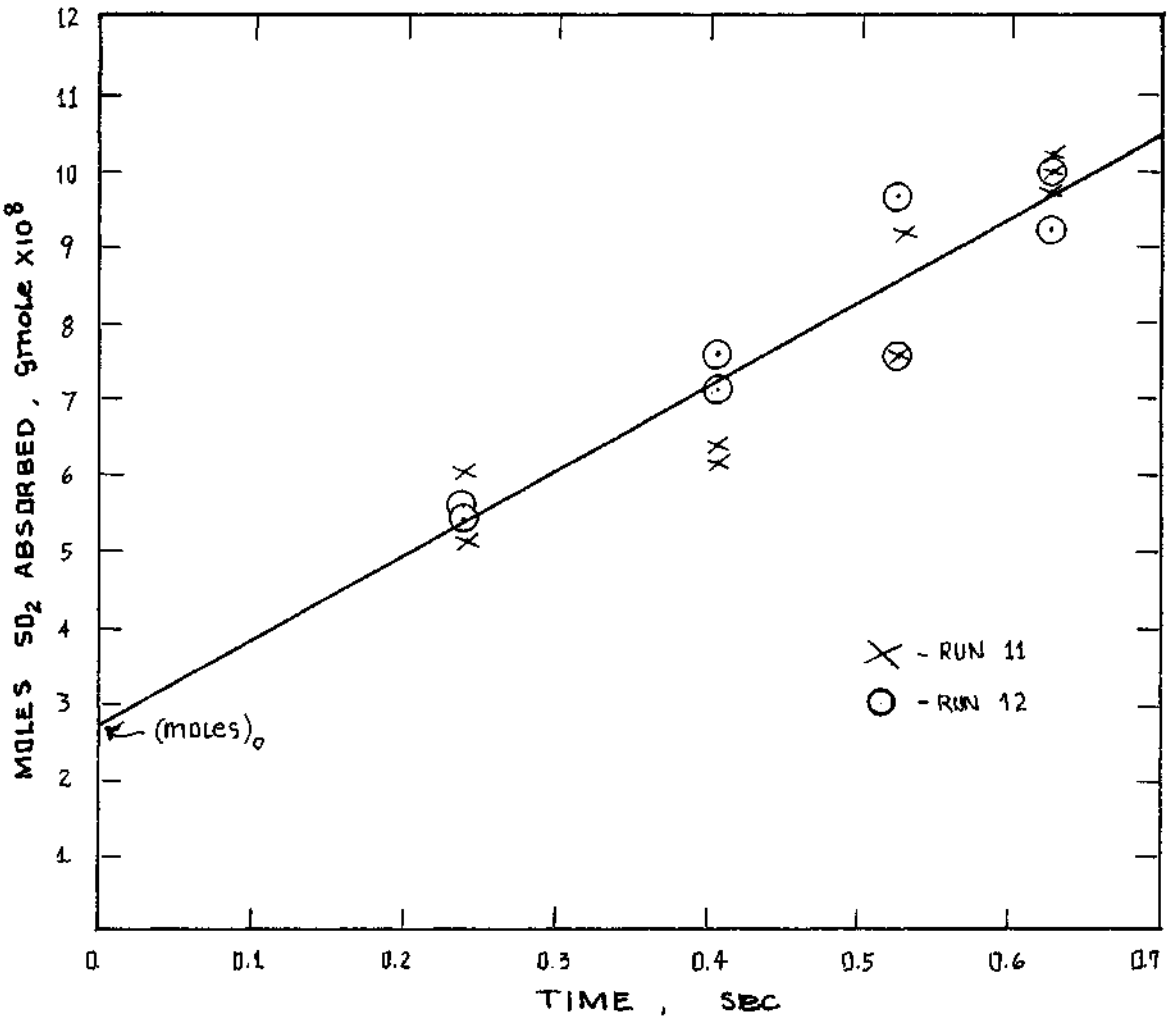

Figure 5. The Effect of Time on SO_2 Absorption (SO_2 = 2000; SSR = 2.0)

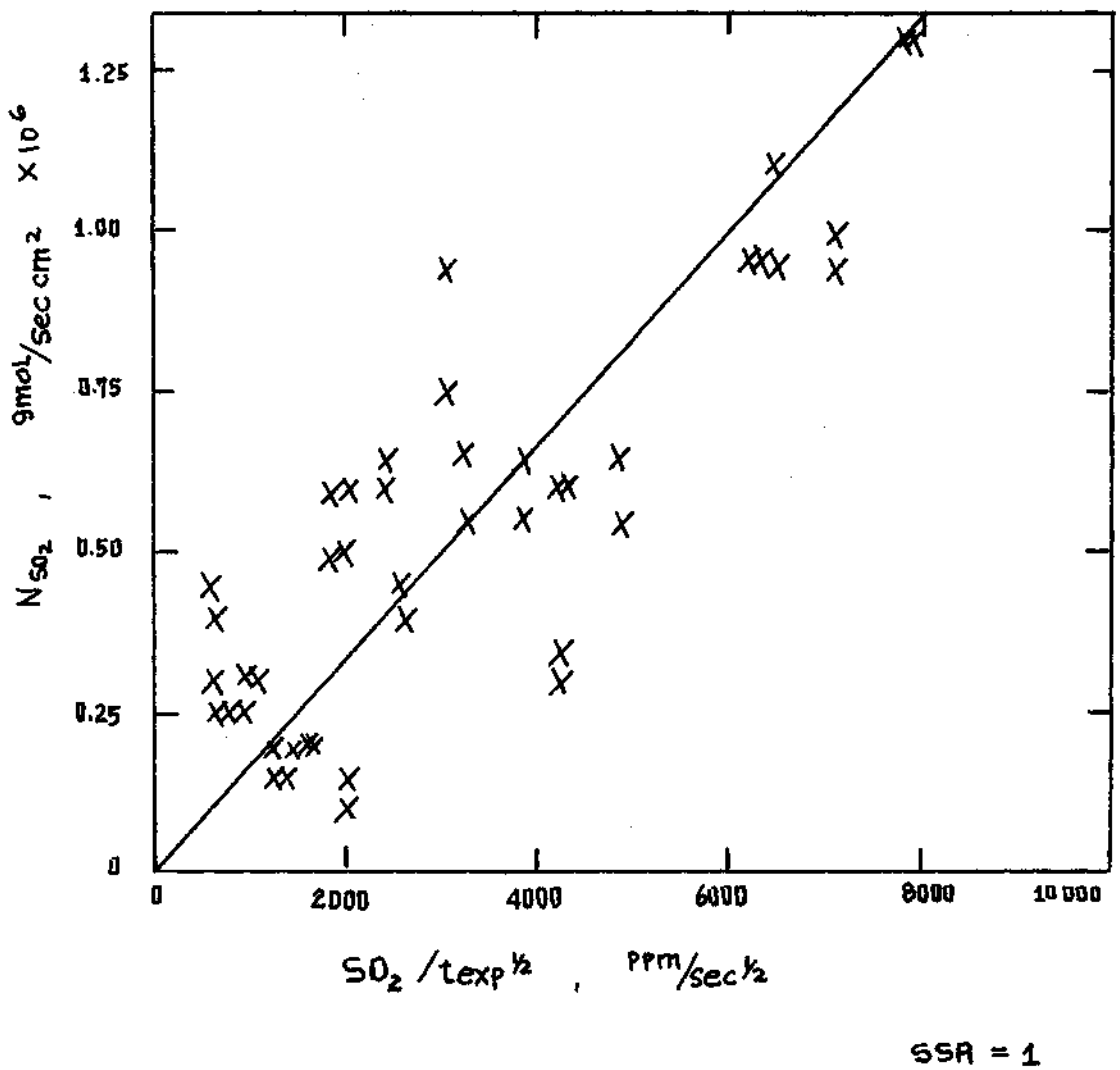

Figure 6. SO_2 Molar Flux versus $SO_2/t_{exp}^{1/2}$

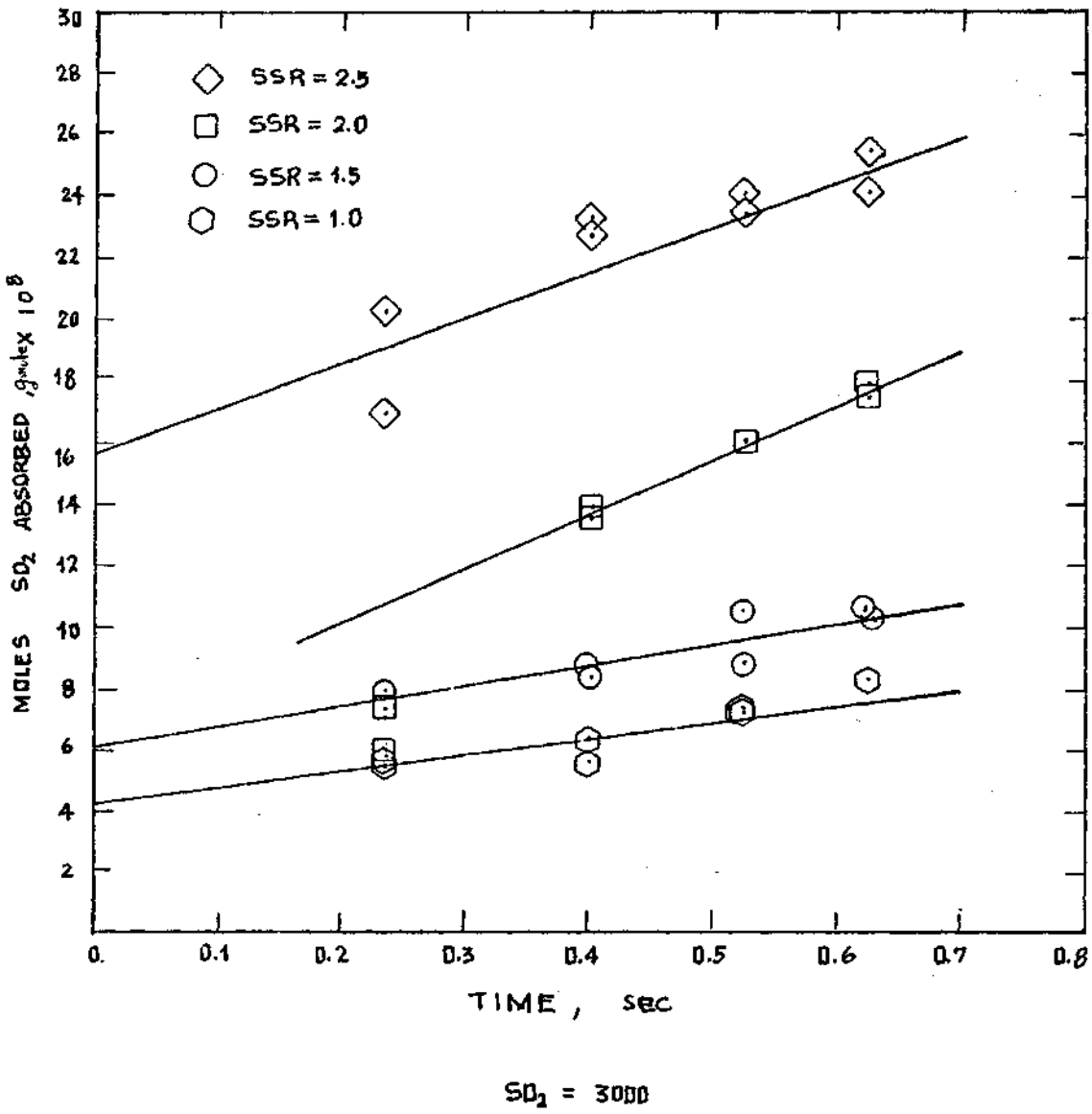

SO_2 = 3000

Figure 7. The Effect of SSR and Time on Moles of SO_2 Absorbed

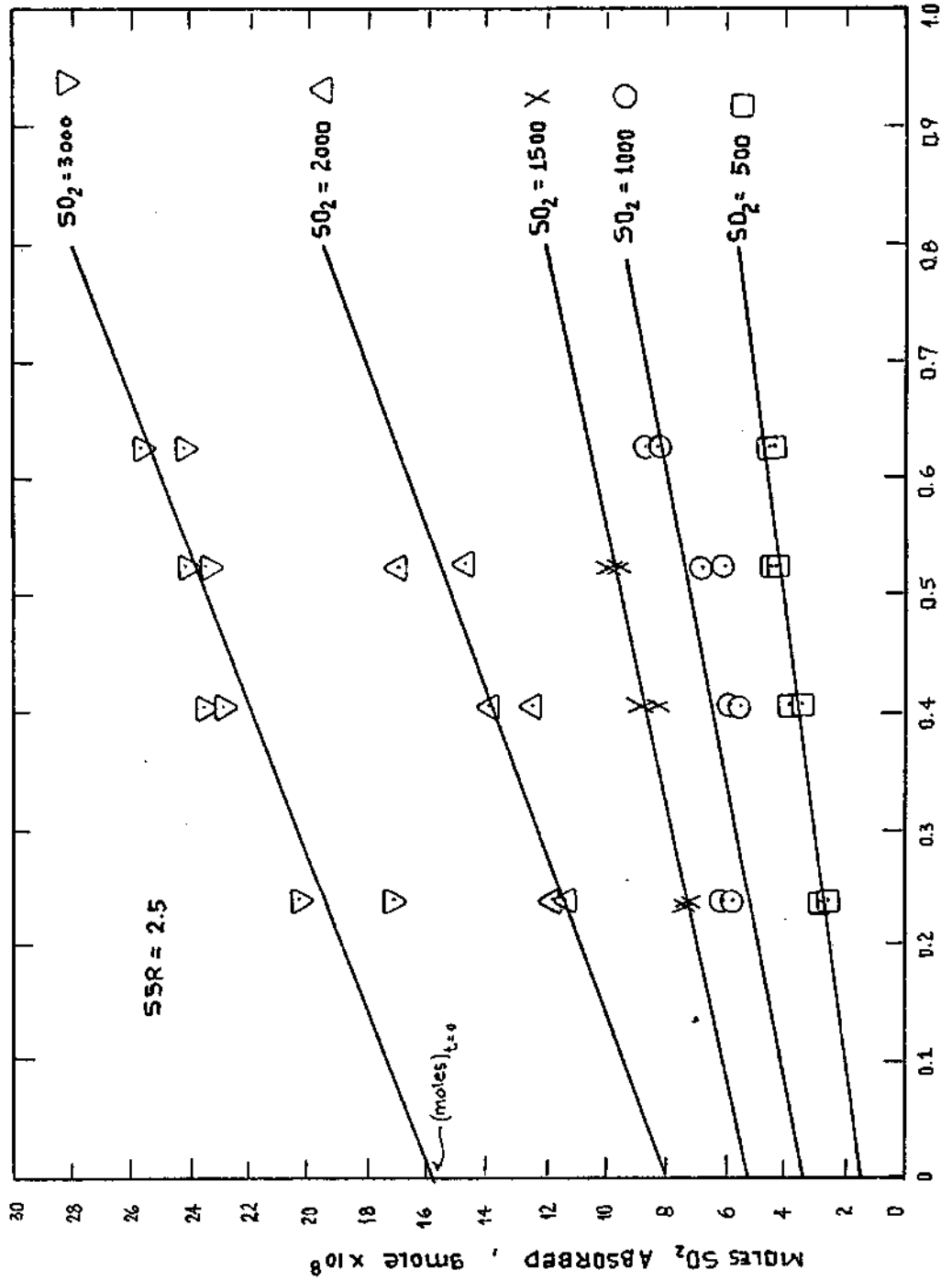

Figure 8. The Effect of Time and SO_2 on Moles of SO_2 Absorbed

and time on absorption at a constant supersaturation ratio (2.5). Both of these figures verify that the absorption is a linear function of time. Since the rate of condensation is a constant, the moles of water condensed are also a linear function of time.

Figure 9 uses a slightly different method to analyze the data. Here the molar flux of SO_2 at a given time is plotted versus time. This indicates that the flux is very high at short exposure time and decreases with time.

By extrapolating the moles of SO_2 absorbed to the intercept at zero exposure time, one can estimate the effects of drop formation and internal circulation. The difference between this number and the moles absorbed at a given time gives the moles absorbed after time zero. Figure 10 is a plot of the flux after time zero versus time. While there is considerable scatter due to subtraction of two numbers with variance, the trend implied is that there is no effect of time on this flux. Again, these data were taken during periods of constant condensation.

Finally, in order to test the prediction (Equation 9) that the absorption is exponentially related to the rate of condensation, Figure 11 was prepared. Again there is some scatter here, but an exponential relation is implied.

The results obtained in this experiment tend to verify the absorption model of Groothius. Also, the pronounced effect on absorption obtainable through condensation of humidity was demonstrated. Finally, the primary objective of this research, to examine the effects of gas phase solute concentration exposure time and supersaturation on the absorption

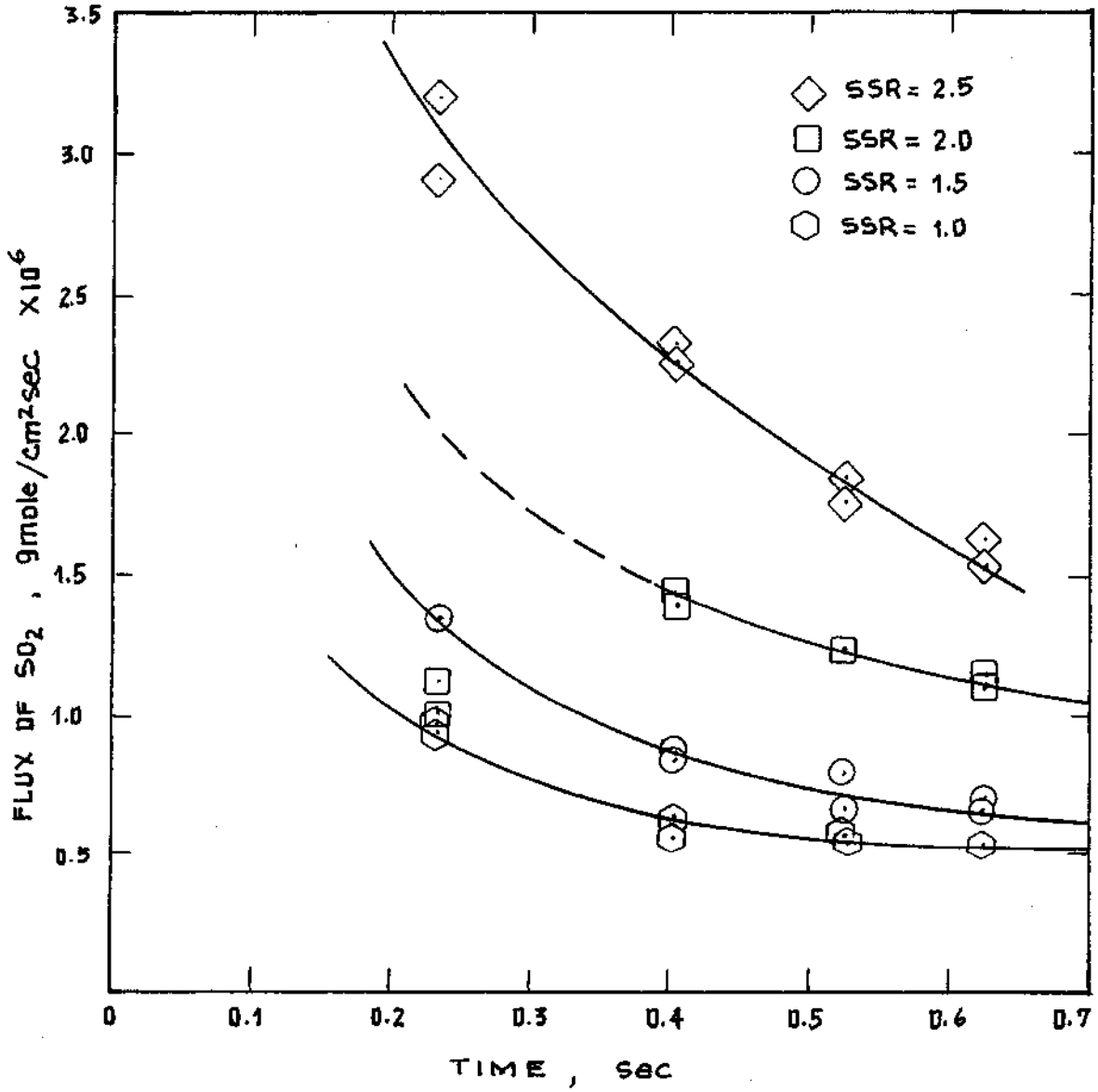

Figure 9. The Effect of Time and SSR on Molar Flux of SO_2 (SO_2 = 3000)

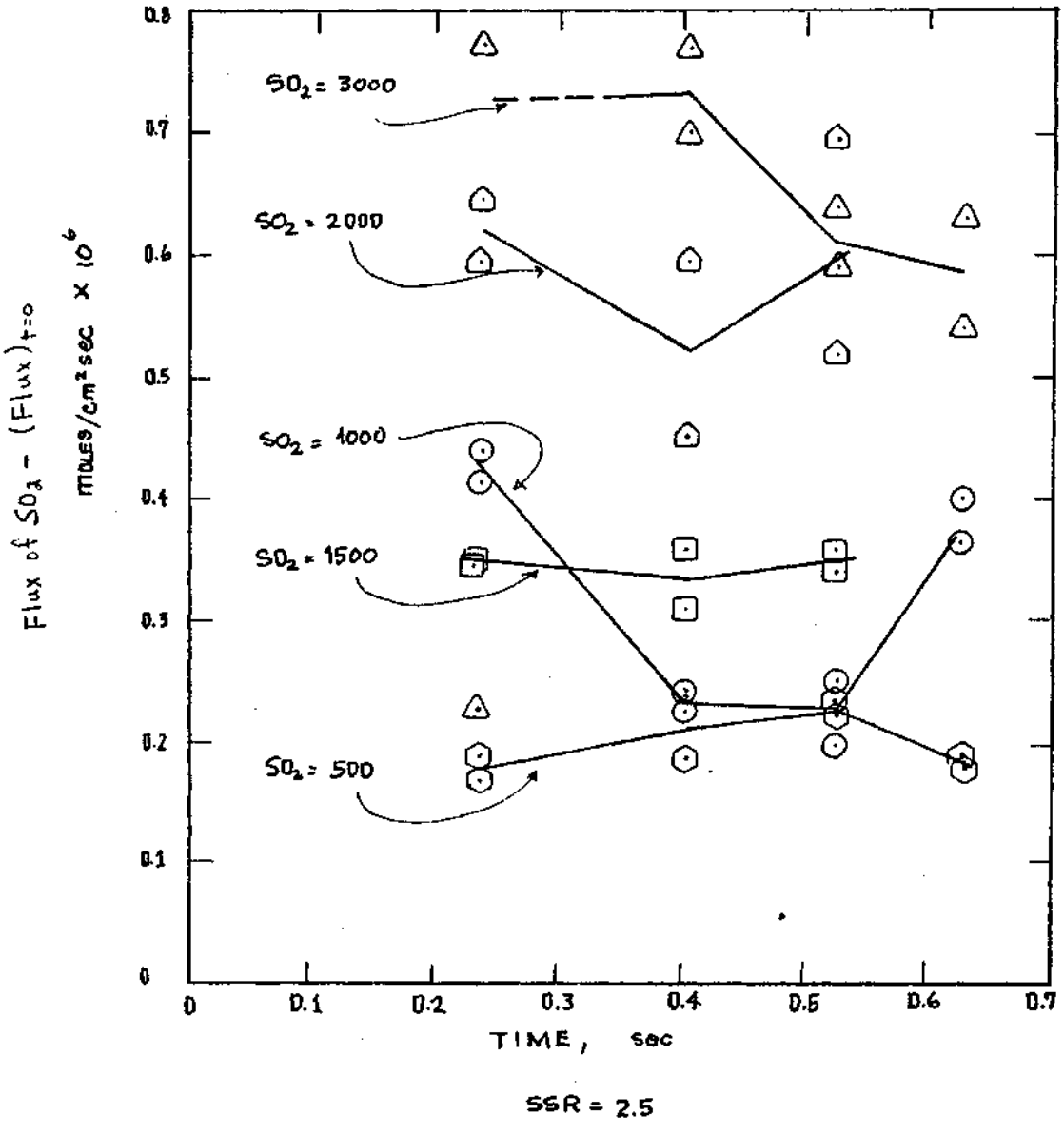

Figure 10. The Effect of Time and SO_2 on Flux-$(Flux)_{t=0}$ of SO_2 Absorbed

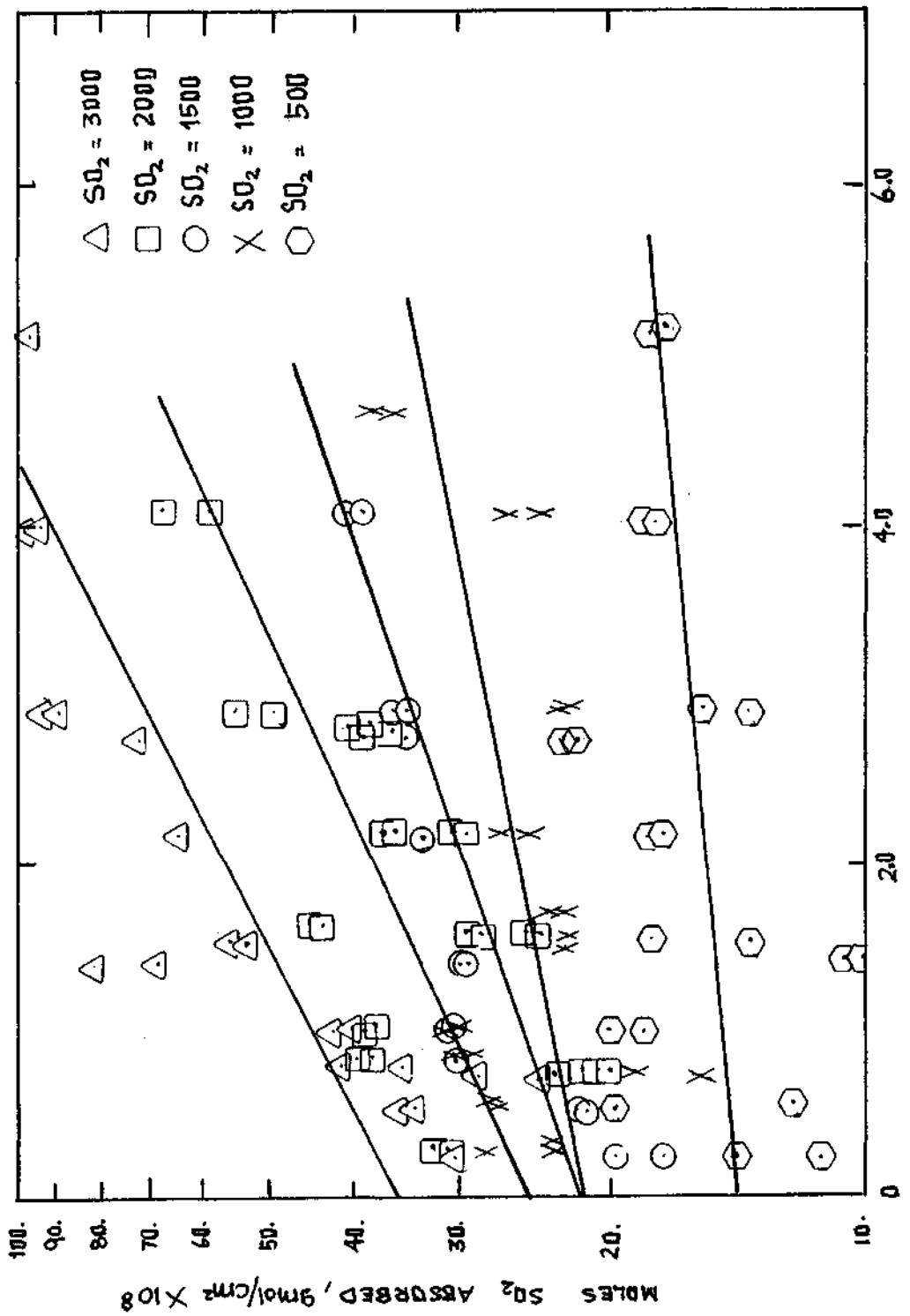

Figure 11. The Effect of Condensation on Absorption of SO_2

of sulfur dioxide by aqueous droplets, was satisfied.

The significance of this effort might be found in a number of areas. First, in industrial scrubbing the effectiveness of a spray tower scrubber, a spray venturi scrubber, or any spray device might be significantly enhanced by the use of a condensing liquid. The increased rate of absorption need not be limited to just sulfur dioxide or just scrubbing, either. Any type of gas-liquid operation where mass transfer across a phase interface is occurring might be enhanced by this phenomenon. Finally, as raindrops fall from the clouds, an area of high humidity, they may acquire additional surface due to condensation in falling through the atmosphere, and, as a result, absorb various gases from the air. This may account for the unusually high quantities of nitrates and sulfates in rainwater.

CHAPTER VI

CONCLUSIONS

In light of the preceding results, the following conclusions may be drawn:

1. The existing theories of absorption are inadequate to describe the process of absorption of a trace gas by a liquid droplet during condensation. All factors point to the surface of the droplet as the source of the inadequacy in theory.

2. The rate of mass transfer increases with increasing gas phase partial pressure, with increasing exposure time, and with increasing condensation rate.

3. The moles per unit area of sulfur dioxide correlate with the moles per unit area of water condensed for supersaturation ratios greater than one.

4. The penetration theory adequately describes the rate of absorption in the absence of condensation.

5. Equation 9 adequately describes the absorption process in the presence of condensation.

CHAPTER VII

RECOMMENDATIONS

From these results, it is expected that condensation of humidity onto a water droplet enhances the rate of absorption of a trace gas such as sulfur dioxide. It still remains to define the precise interrelationship among surface effects, adsorption-desorption rates, exposure time, and condensation rate over a continuous spectrum of values. Further research may yield results of value in systems for pollution control as well as helping to explain the synergism seen between trace gaseous pollutants and aerosols. Also, the effects of surface tension, solubility, and the presence of liquid phase reaction are yet to be determined. Work in this area is recommended.

APPENDIX A

NOMENCLATURE

A	arbitrary constant
C	concentration, gmol/cm^3
C_{AO}	initial concentration of A, gmol/cm^3
C_{AS}	concentration of A at the surface, gmol/cm^3
C_A	concentration of A in the bulk phase, gmol/cm^3
C_D	drag coefficient, dimensionless
C^2	inverse of terminal velocity, sec/cm
C_P	heat capacity, cal/g°C
D_{AB}	diffusivity of A in B, cm^2/sec
D_{H_2O}	diffusivity of water in N_2, cm^2/sec
DR	drop rate, drops/min
D_P	drop diameter, cm
g	acceleration due to gravity, cm/sec^2
h	heat transfer coefficient, cal/cm^2-sec-°K
H_A	Henry's law constant, (gmol/cm^3)/atm
K_x	mass transfer coefficient, gmol/cm^2-sec mm Hg
K	thermal conductivity, cal/cm^2-sec-°C/cm
k	proportionality constant
λ	heat of condensation, cal/g
m	mass, g
M_A	molecular weight of A, g/gmol

μ	viscosity, g/cm-sec
μ_{N_2}	viscosity of nitrogen, g/cm-sec
μ_D	viscosity of the drop, g/cm-sec
N_A	flux of A, gmol/cm^2-sec
Nu	Nusselt number, dimensionless
ν	velocity, cm/sec
ν_+	terminal velocity, cm/sec
P	total pressure, mm Hg
$\overline{P}_A$	partial pressure of A, mm Hg
P_{sat}	saturation partial pressure of water, mm Hg
P_{01}	vapor pressure of water, mm Hg
$\overline{P}_W$	partial pressure of water, mm Hg
Q	heat transfer rate, cal/sec
R	gas law constant, (cm^3 mm Hg)/gmol-°K
R_P	radius of a drop, cm
Re	Reynolds number, dimensionless
R_{SF}	flux due to Stephan flow, gmol/cm^2/sec
R_{KE}	flux due to kinetic energy, gmol/cm^2-sec
ρ	density, g/cm^3
ρ_D	density of drops, g/cm^3
ρ_{N_2}	density of nitrogen, g/cm^3
ρ_{AS}	density of A at the surface, g/cm^3
S	surface area, cm^2
Sc	Schmidt number, dimensionless
Sh	Sherwood number, dimensionless

S_0	initial surface area, cm^2
SSR	supersaturation ratio, dimensionless
SO_2	gas phase sulfur dioxide concentration, ppm
SO_4	liquid phase sulfate concentration, normal
t	time, sec
t_{exp}	exposure time, sec
T	temperature, °K
T_D	temperature of drop, °C
T_{N_2}	temperature of nitrogen, °C
T_{H_2O}	temperature of the drop at the needle, °C
T_{sample}	temperature of the drop as collected, °C
T_{wb}	wet bulb temperature, °C
T_{db}	dry bulb temperature, °C
V	drop volume, cm^3
v	water flow rate, cm^3/min
W	rate of water condensed, g/sec
X	distance, cm
X_2	effective film thickness, cm

APPENDIX B

EXPERIMENTALLY MEASURED DATA

Table 2. Experimentally Measured Data for Sulfur Dioxide

No.	Case	Length cm	SO_2 Conc. ppm	pH	T_{db} °C	T_{wb} °C	T_{H_2O} °C	T_{sample} °C	H_2O Flow Rate cm^3/min	DR drops/min
1	1	177.	0.	5.80	21.1	12.8	7.0	9.0	2.014	2.86
2	1	177.	0.	5.90	21.1	12.8	7.0	9.0	2.014	2.86
3	2	177.	1000.	2.60	21.1	12.8	7.0	9.0	2.014	2.86
4	2	177.	1000.	2.69	21.1	12.8	7.0	9.0	2.014	2.86
5	2	127.	1000.	2.75	21.1	12.8	7.0	9.0	2.014	2.86
6	2	127.	1000.	2.73	21.1	12.8	7.0	9.0	2.014	2.86
7	2	77.	1000.	2.80	21.1	12.8	7.0	9.0	2.014	2.86
8	2	77.	1000.	2.81	21.1	12.8	7.0	9.0	2.014	2.86
9	2	27.	1000.	3.24	21.1	12.8	7.0	9.0	2.014	2.86
10	2	27.	1000.	3.14	21.1	12.8	7.0	9.0	2.014	2.86
11	3	27.	2000.	2.79	21.1	12.8	7.0	9.0	2.014	2.86
12	3	27.	2000.	2.83	21.1	12.8	7.0	9.0	2.014	2.86
13	3	77.	2000.	2.41	21.1	12.8	7.0	9.0	2.014	2.86
14	3	77.	2000.	2.36	21.1	12.8	7.0	9.0	2.014	2.86
15	3	127.	2000.	2.60	21.1	12.8	7.0	9.0	2.014	2.86
16	3	127.	2000.	2.51	21.1	12.8	7.0	9.0	2.014	2.86
17	3	177.	2000.	2.36	21.1	12.8	7.0	9.0	2.014	2.86
18	3	177.	2000.	2.32	21.1	12.8	7.0	9.0	2.014	2.86
19	4	177.	3000.	2.26	21.1	12.8	7.0	9.0	2.014	2.86
20	4	177.	3000.	2.19	21.1	12.8	7.0	9.0	2.014	2.86
21	4	127.	3000.	2.30	21.1	12.8	7.0	9.0	2.014	2.86
22	4	127.	3000.	2.30	21.1	12.8	7.0	9.0	2.014	2.86
23	4	77.	3000.	2.40	21.1	12.8	7.0	9.0	3.014	2.86
24	4	77.	3000.	2.36	21.1	12.8	7.0	9.0	2.014	2.86
25	4	27.	3000.	2.40	21.1	12.8	7.0	9.0	2.014	2.86
26	4	27.	3000.	2.41	21.1	12.8	7.0	9.0	2.014	2.86
27	5	27.	5000.	2.10	21.1	12.8	7.0	9.0	2.014	2.86
28	5	27.	5000.	2.08	21.1	12.8	7.0	9.0	2.014	2.86

Table 2. Continued

No.	Case	Length cm	SO_2 Conc. ppm	pH	T_{db} °C	T_{wb} °C	T_{H_2O} °C	T_{sample} °C	H_2O Flow Rate cm^3/min	DR drops/min
29	5	77.	5000.	2.10	21.1	12.8	7.0	9.0	2.014	2.86
30	5	77.	5000.	2.10	21.1	12.8	7.0	9.0	2.014	2.86
31	5	127.	5000.	2.12	21.1	12.8	7.0	9.0	2.014	2.86
32	5	127.	5000.	2.10	21.1	12.8	7.0	9.0	2.014	2.86
33	5	177.	5000.	2.06	21.1	12.8	7.0	9.0	2.014	2.86
34	5	177.	5000.	2.01	21.1	12.8	7.0	9.0	2.014	2.86
35	6	27.	500.	2.88	21.1	12.8	7.0	9.0	2.014	2.86
36	6	27.	500.	2.86	21.1	12.8	7.0	9.0	2.014	2.86
37	6	77.	500.	2.69	21.1	12.8	7.0	9.0	2.014	2.86
38	6	77.	500.	2.70	21.1	12.8	7.0	9.0	2.014	2.86
39	6	127.	500.	2.57	21.1	12.8	7.0	9.0	2.014	2.86
40	6	127.	500.	2.58	21.1	12.8	7.0	9.0	2.014	2.86
41	6	177.	500.	2.37	21.1	12.8	7.0	9.0	2.014	2.86
42	6	177.	500.	2.31	21.1	12.8	7.0	9.0	2.014	2.86
43	7	177.	1500.	2.29	21.1	12.8	7.0	9.0	2.014	2.86
44	7	177.	1500.	2.23	21.1	12.8	7.0	9.0	2.014	2.86
45	7	127.	1500.	2.30	21.1	12.8	7.0	9.0	2.014	2.86
46	7	127.	1500.	2.34	21.1	12.8	7.0	9.0	2.014	2.86
47	7	77.	1500.	2.35	21.1	12.8	7.0	9.0	2.014	2.86
48	7	77.	1500.	2.37	21.1	12.8	7.0	9.0	2.014	2.86
49	7	27.	1500.	2.50	21.1	12.8	7.0	9.0	2.014	2.86
50	7	27.	1500.	2.41	21.1	12.8	7.0	9.0	2.014	2.86
51	8	27.	500.	2.94	22.2	19.4	7.0	9.0	2.014	2.86
52	8	27.	500.	2.87	22.2	19.4	7.0	9.0	2.014	2.86
53	8	77.	500.	2.49	22.2	19.4	7.0	9.0	2.014	2.86
54	8	77.	500.	2.59	22.2	19.4	7.0	9.0	2.014	2.86
55	8	127.	500.	2.50	22.2	19.4	7.0	9.0	2.014	2.86
56	8	127.	500.	2.49	22.2	19.4	7.0	9.0	2.014	2.86
57	8	177.	500.	2.41	22.2	19.4	7.0	9.0	2.014	2.86

Table 2. Continued

No.	Case	Length cm	SO_2 Conc. ppm	pH	T_{db} °C	T_{wb} °C	T_{H_2O} °C	T_{sample} °C	H_2O Flow Rate cm^3/min	DR drops/min
58	8	177.	500.	2.40	22.2	19.4	7.0	9.0	2.014	2.86
59	9	177.	1000.	2.80	22.2	19.4	7.0	9.0	2.014	2.86
60	9	177.	1000.	2.75	22.2	19.4	7.0	9.0	2.014	2.86
61	9	127.	1000.	2.36	22.2	19.4	7.0	9.0	2.014	2.86
62	9	127.	1000.	2.33	22.2	19.4	7.0	9.0	2.014	2.86
63	9	77.	1000.	2.40	22.2	19.4	7.0	9.0	2.014	2.86
64	9	77.	1000.	2.40	22.2	19.4	7.0	9.0	2.014	2.86
65	9	27.	1000.	2.51	22.2	19.4	7.0	9.0	2.014	2.86
66	9	27.	1000.	2.47	22.2	19.4	7.0	9.0	2.014	2.86
67	10	27.	1500.	2.44	22.2	19.4	7.0	9.0	2.014	2.86
68	10	27.	1500.	2.49	22.2	19.4	7.0	9.0	2.014	2.86
69	10	77.	1500.	2.59	22.2	19.4	7.0	9.0	2.014	2.86
70	10	77.	1500.	2.61	22.2	19.4	7.0	9.0	2.014	2.86
71	10	127.	1500.	2.27	22.2	19.4	7.0	9.0	2.014	2.86
72	10	127.	1500.	2.29	22.2	19.4	7.0	9.0	2.014	2.86
73	10	177.	1500.	2.25	22.2	19.4	7.0	9.0	2.014	2.86
74	10	177.	1500.	2.23	22.2	19.4	7.0	9.0	2.014	2.86
75	11	177.	2000.	2.21	22.2	19.4	7.0	9.0	2.014	2.86
76	11	177.	2000.	2.20	22.2	19.4	7.0	9.0	2.014	2.86
77	11	127.	2000.	2.23	22.2	19.4	7.0	9.0	2.014	2.86
78	11	127.	2000.	2.30	22.2	19.4	7.0	9.0	2.014	2.86
79	11	77.	2000.	2.36	22.2	19.4	7.0	9.0	2.014	2.86
80	11	77.	2000.	2.37	22.2	19.4	7.0	9.0	2.014	2.86
81	11	27.	2000.	2.38	22.2	19.4	7.0	9.0	2.014	2.86
82	11	27.	2000.	2.44	22.2	19.4	7.0	9.0	2.014	2.86
83	11	177.	2000.	2.19	22.2	19.4	7.0	9.0	2.014	2.86
84	12	27.	2000.	2.41	22.2	19.4	7.0	9.0	2.014	2.86
85	12	27.	2000.	2.42	22.2	19.4	7.0	9.0	2.014	2.86
86	12	77.	2000.	2.30	22.2	19.4	7.0	9.0	2.014	2.86

Table 2. Continued

No.	Case	Length cm	SO_2 Conc. ppm	pH	T_{db} °C	T_{wb} °C	T_{H_2O} °C	T_{sample} °C	H_2O Flow Rate cm^3/min	DR drops/min
87	12	77.	2000.	2.32	22.2	19.4	7.0	9.0	2.014	2.86
88	12	127.	2000.	2.30	22.2	19.4	7.0	9.0	2.014	2.86
89	12	127.	2000.	2.21	22.2	19.4	7.0	9.0	2.014	2.86
90	12	177.	2000.	2.20	22.2	19.4	7.0	9.0	2.014	2.86
91	12	177.	2000.	2.23	22.2	19.4	7.0	9.0	2.014	2.86
92	13	177.	3000.	1.99	22.2	19.4	7.0	9.0	2.014	2.86
93	13	177.	3000.	2.00	22.2	19.4	7.0	9.0	2.014	2.86
94	13	127.	3000.	2.03	22.2	19.4	7.0	9.0	2.014	2.86
95	13	127.	3000.	2.10	22.2	19.4	7.0	9.0	2.014	2.86
96	13	77.	3000.	2.08	22.2	19.4	7.0	9.0	2.014	2.86
97	13	77.	3000.	2.09	22.2	19.4	7.0	9.0	2.014	2.86
98	13	27.	3000.	2.31	22.2	19.4	7.0	9.0	2.014	2.86
99	13	27.	3000.	2.38	22.2	19.4	7.0	9.0	2.014	2.86
100	14	27.	500.	2.69	21.7	20.6	7.0	9.0	2.014	2.86
101	14	27.	500.	2.71	21.7	20.6	7.0	9.0	2.014	2.86
102	14	77.	500.	2.54	21.7	20.6	7.0	9.0	2.014	2.86
103	14	77.	500.	2.59	21.7	20.6	7.0	9.0	2.014	2.86
104	14	127.	500.	2.48	21.7	20.6	7.0	9.0	2.014	2.86
105	14	127.	500.	2.49	21.7	20.6	7.0	9.0	2.014	2.86
106	14	177.	500.	2.50	21.7	20.6	7.0	9.0	2.014	2.86
107	14	177.	500.	2.49	21.7	20.6	7.0	9.0	2.014	2.86
108	15	177.	1000.	2.21	21.7	20.6	7.0	9.0	2.014	2.86
109	15	177.	1000.	2.23	21.7	20.6	7.0	9.0	2.014	2.86
110	15	127.	1000.	2.38	21.7	20.6	7.0	9.0	2.014	2.86
111	15	127.	1000.	2.34	21.7	20.6	7.0	9.0	2.014	2.86
112	15	77.	1000.	2.40	21.7	20.6	7.0	9.0	2.014	2.86
113	15	77.	1000.	2.39	21.7	20.6	7.0	9.0	2.014	2.86
114	15	27.	1000.	2.38	21.7	20.6	7.0	9.0	2.014	2.86

Table 2. Continued

No.	Case	Length cm	SO_2 Conc. ppm	pH	T_{db} °C	T_{wb} °C	T_{H_2O} °C	T_{sample} °C	H_2O Flow Rate cm^3/min	DR drops/min
115	15	27.	1000.	2.39	21.7	20.6	7.0	9.0	2.014	2.86
116	16	27.	1500.	2.31	21.7	20.6	7.0	9.0	2.014	2.86
117	16	27.	1500.	2.31	21.7	20.6	7.0	9.0	2.014	2.86
118	16	77.	1500.	2.24	21.7	20.6	7.0	9.0	2.014	2.86
119	16	77.	1500.	2.26	21.7	20.6	7.0	9.0	2.014	2.86
120	16	127.	1500.	2.21	21.7	20.6	7.0	9.0	2.014	2.86
121	16	127.	1500.	2.20	21.7	20.6	7.0	9.0	2.014	2.86
122	16	177.	1500.	2.28	21.7	20.6	7.0	9.0	2.014	2.86
123	16	177.	1500.	2.28	21.7	20.6	7.0	9.0	2.014	2.86
124	17	177.	2000.	2.41	21.7	20.6	7.0	9.0	2.014	2.86
125	17	177.	2000.	2.43	21.7	20.6	7.0	9.0	2.014	2.86
126	17	127.	2000.	2.01	21.7	20.6	7.0	9.0	2.014	2.86
127	17	127.	2000.	2.06	21.7	20.6	7.0	9.0	2.014	2.86
128	17	77.	2000.	2.08	21.7	20.6	7.0	9.0	2.014	2.86
129	17	77.	2000.	2.12	21.7	20.6	7.0	9.0	2.014	2.86
130	17	27.	2000.	2.15	21.7	20.6	7.0	9.0	2.014	2.86
131	17	27.	2000.	2.14	21.7	20.6	7.0	9.0	2.014	2.86
132	18	27.	3000.	2.01	21.7	20.6	7.0	9.0	2.014	2.86
133	18	27.	3000.	1.95	21.7	20.6	7.0	9.0	2.014	2.86
134	18	77.	3000.	1.90	21.7	20.6	7.0	9.0	2.014	2.86
135	18	77.	3000.	1.91	21.7	20.6	7.0	9.0	2.014	2.86
136	18	127.	3000.	1.89	21.7	20.6	7.0	9.0	2.014	2.86
137	18	127.	3000.	1.90	21.7	20.6	7.0	9.0	2.014	2.86
138	18	177.	3000.	1.87	21.7	20.6	7.0	9.0	2.014	2.86
139	18	177.	3000.	1.89	21.7	20.6	7.0	9.0	2.014	2.86
140	19	177.	500.	2.48	21.1	16.1	7.0	9.0	2.014	2.86
141	19	177.	500.	2.44	21.1	16.1	7.0	9.0	2.014	2.86
142	19	127.	500.	2.52	21.1	16.1	7.0	9.0	2.014	2.86
143	19	127.	500.	2.51	21.1	16.1	7.0	9.0	2.014	2.86

Table 2. Continued

No.	Case	Length cm	SO_2 Conc. ppm	pH	T_{db} °C	T_{wb} °C	T_{H_2O} °C	T_{sample} °C	H_2O Flow Rate cm^3/min	DR drops/min
144	19	77.	500.	2.45	21.1	16.1	7.0	9.0	2.014	2.86
145	19	77.	500.	2.63	21.1	16.1	7.0	9.0	2.014	2.86
146	19	27.	500.	2.57	21.1	16.1	7.0	9.0	2.014	2.86
147	19	27.	500.	2.66	21.1	16.1	7.0	9.0	2.014	2.86
148	20	27.	1000.	2.39	21.1	16.1	7.0	9.0	2.014	2.86
149	20	27.	1000.	2.32	21.1	16.1	7.0	9.0	2.014	2.86
150	20	77.	1000.	2.32	21.1	16.1	7.0	9.0	2.014	2.86
151	20	77.	1000.	2.32	21.1	16.1	7.0	9.0	2.014	2.86
152	20	127.	1000.	2.29	21.1	16.1	7.0	9.0	2.014	2.86
153	20	127.	1000.	2.26	21.1	16.1	7.0	9.0	2.014	2.86
154	20	177.	1000.	2.40	21.1	16.1	7.0	9.0	2.014	2.86
155	20	177.	1000.	2.29	21.1	16.1	7.0	9.0	2.014	2.86
156	21	177.	1500.	2.30	21.1	16.1	7.0	9.0	2.014	2.86
157	21	177.	1500.	2.30	21.1	16.1	7.0	9.0	2.014	2.86
158	21	127.	1500.	2.30	21.1	16.1	7.0	9.0	2.014	2.86
159	21	127.	1500.	2.41	21.1	16.1	7.0	9.0	2.014	2.86
160	21	77.	1500.	2.42	21.1	16.1	7.0	9.0	2.014	2.86
161	21	77.	1500.	2.43	21.1	16.1	7.0	9.0	2.014	2.86
162	21	27.	1500.	2.51	21.1	16.1	7.0	9.0	2.014	2.86
163	21	27.	1500.	2.46	21.1	16.1	7.0	9.0	2.014	2.86
164	22	27.	2000.	2.26	21.1	16.1	7.0	9.0	2.014	2.86
165	22	27.	2000.	2.27	21.1	16.1	7.0	9.0	2.014	2.86
166	22	77.	2000.	2.12	21.1	16.1	7.0	9.0	2.014	2.86
167	22	77.	2000.	2.14	21.1	16.1	7.0	9.0	2.014	2.86
168	22	127.	2000.	2.21	21.1	16.1	7.0	9.0	2.014	2.86
169	22	127.	2000.	2.20	21.1	16.1	7.0	9.0	2.014	2.86
170	22	177.	2000.	2.21	21.1	16.1	7.0	9.0	2.014	2.86
171	22	177.	2000.	2.20	21.1	16.1	7.0	9.0	2.014	2.86
172	23	177.	3000.	2.18	21.1	16.1	7.0	9.0	2.014	2.86

Table 2. Concluded

No.	Case	Length cm	SO_2 Conc. ppm	pH	T_{db} °C	T_{wb} °C	T_{H_2O} °C	T_{sample} °C	H_2O Flow Rate cm^3/min	DR drops/min
173	23	177.	3000.	2.19	21.1	16.1	7.0	9.0	2.014	2.86
174	23	127.	3000.	2.24	21.1	16.1	7.0	9.0	2.014	2.86
175	23	127.	3000.	2.18	21.1	16.1	7.0	9.0	2.014	2.86
176	23	77.	3000.	2.25	21.1	16.1	7.0	9.0	2.014	2.86
177	23	77.	3000.	2.26	21.1	16.1	7.0	9.0	2.014	2.86
178	23	27.	3000.	2.06	21.1	16.1	7.0	9.0	2.014	2.86
179	23	27.	3000.	2.28	21.1	16.1	7.0	9.0	2.014	2.86

Table 3. Experimentally Measured Data for Oxygen Absorption

Run No.	T_{db} °C	T_{wb} °C	Length cm	O_2 Vol %	Microgasmeter initial mm Hg	$\bar{p}\ O_2$ final mm Hg
1	21.1	15.0	177	5	8.65	9.42
2	21.1	15.0	177	10	9.16	9.68
3	21.1	15.0	177	15	9.04	8.46
4	21.1	15.0	177	21	8.16	8.18
5	21.1	15.0	127	21	9.04	8.26
6	21.1	15.0	127	15	8.22	8.31
7	21.1	15.0	127	10	7.60	8.00
8	21.1	15.0	127	5	9.50	9.61
9	21.1	15.0	77	5	8.30	8.95
10	21.1	15.0	77	10	8.46	8.18
11	21.1	15.0	77	15	8.81	8.81
12	21.1	15.0	77	21	9.62	9.51
13	21.1	15.0	27	21	8.85	9.17
14	21.1	15.0	27	15	8.91	9.27
15	21.1	15.0	27	10	8.18	8.40
16	21.1	15.0	27	5	9.31	9.77
17	21.1	12.2	27	5	9.61	8.88
18	21.1	12.2	27	10	8.65	8.71
19	21.1	12.2	27	15	9.62	9.98
20	21.1	12.2	27	21	9.10	9.10
21	21.1	12.2	77	21	8.65	7.48
22	21.1	12.2	77	15	7.61	8.01
23	21.1	12.2	77	10	8.31	8.86
24	21.1	12.2	77	5	8.51	8.51
25	21.1	12.2	127	5	7.69	8.69
26	21.1	12.2	127	10	8.41	8.65
27	21.1	12.2	127	15	8.91	9.20
28	21.1	12.2	127	21	9.31	9.41
29	21.1	12.2	177	21	9.40	9.51
30	21.1	12.2	177	15	9.61	9.87
32	21.1	12.2	177	5	8.41	9.36
33	21.1	17.8	177	5	8.04	8.61
34	21.1	17.8	177	10	8.92	9.21
35	21.1	17.8	177	15	9.44	9.60
36	21.1	17.8	177	21	9.31	9.36
37	21.1	17.8	127	21	6.21	7.41
38	21.1	17.8	127	15	7.00	7.62
39	21.1	17.8	127	10	8.44	9.10
40	21.1	17.8	127	5	9.66	9.32

Table 3. Concluded

Run No.	T_{db} °C	T_{wb} °C	Length cm	O_2 Vol %	Microgasmeter initial mm Hg	$\bar{p}\ O_2$ final mm Hg
41	21.1	17.8	77	5	8.17	8.26
42	21.1	17.8	77	10	8.94	8.83
43	21.1	17.8	77	15	9.41	8.06
44	21.1	17.8	77	21	9.44	9.69
45	21.1	17.8	27	21	8.44	8.21
46	21.1	17.8	27	15	8.96	9.44
47	21.1	17.8	27	10	9.62	9.83
48	21.1	17.8	27	5	9.02	9.81
49	21.7	20.6	27	5	6.44	6.64
50	21.7	20.6	27	10	7.21	7.18
51	21.7	20.6	27	15	8.66	8.94
52	21.7	20.6	27	21	7.21	7.41
53	21.7	20.6	77	21	9.26	9.44
54	21.7	20.6	77	15	9.29	9.62
55	21.7	20.6	77	10	9.49	9.86
56	21.7	20.6	77	5	9.04	9.22
57	21.7	20.6	127	5	4.45	4.96
58	21.7	20.6	127	10	4.82	4.01
59	21.7	20.6	127	15	8.21	8.27
60	21.7	20.6	127	21	8.86	8.19
61	21.7	20.6	177	21	9.26	9.84
62	21.7	20.6	177	15	9.18	10.26
63	21.7	20.6	177	10	8.61	8.72
64	21.7	20.6	177	5	8.04	7.62
65	21.1	17.8	177	0	8.95	8.65
66	21.1	17.8	0	0	8.61	8.93

APPENDIX C

CALCULATED VALUES

Table 4. Calculated Values for Sulfur Dioxide

No.	Case	T_{exp} sec	Re	SSR	SO_4 N	Moles SO_2 Absorbed/cm^2 x 10^8	N_{SO_2} x 10^6 mol/cm^2-sec	$SO_2/t_{exp}^{1/2}$ ppm/$sec^{1/2}$
3	2	0.6272	1107.9	1.0	0.00574	13.48	0.2149	1.263
4	2	0.6272	1107.9	1.0	0.00453	10.65	0.1698	1.263
5	2	0.5250	970.7	1.0	0.00388	9.12	0.1736	1.380
6	2	0.5250	970.7	1.0	0.00409	9.60	0.1828	1.380
7	2	0.4039	782.5	1.0	0.00341	8.02	0.1985	1.573
8	2	0.4039	782.5	1.0	0.00333	7.81	0.1935	1.573
9	2	0.2363	480.2	1.0	0.00115	2.70	0.1142	2.057
10	2	0.2363	480.2	1.0	0.00146	3.43	0.1453	2.057
11	3	0.2363	480.2	1.0	0.00350	8.22	0.3481	4.114
12	3	0.2363	480.2	1.0	0.00316	7.43	0.3142	4.114
13	3	0.4039	782.5	1.0	0.00954	22.41	0.5548	3.147
14	3	0.4039	782.5	1.0	0.01093	25.67	0.6357	3.147
17	3	0.6272	1107.9	1.0	0.01093	25.67	0.4094	2.525
18	3	0.6272	1107.9	1.0	0.01220	28.65	0.4567	2.525
19	4	0.6272	1107.9	1.0	0.01439	33.80	0.5390	3.788
20	4	0.6272	1107.9	1.0	0.01749	41.08	0.6549	3.788
21	4	0.5250	970.7	1.0	0.01289	30.27	0.5765	4.140
22	4	0.5250	970.7	1.0	0.01289	30.27	0.5765	4.140
23	4	0.4039	782.5	1.0	0.00980	23.02	0.5701	4.720
24	4	0.4039	782.5	1.0	0.01093	25.67	0.6357	4.720
25	4	0.2363	480.2	1.0	0.00980	23.02	0.9744	6.171
26	4	0.2363	480.2	1.0	0.00954	22.41	0.9483	6.171
27	5	0.2363	480.2	1.0	0.02253	52.92	2.2395	10.286
28	5	0.2363	480.2	1.0	0.02385	56.01	2.3702	10.286
29	5	0.4039	782.5	1.0	0.02253	52.92	1.3102	7.867
30	5	0.4039	782.5	1.0	0.02253	52.92	1.3102	7.867
31	5	0.5250	970.7	1.0	0.02129	50.01	0.9526	6.901
32	5	0.5250	970.7	1.0	0.02253	52.92	1.0080	6.901
33	5	0.6272	1107.9	1.0	0.02524	59.29	0.9453	6.313

Table 4. Continued

No.	Case	T_{exp} sec	Re	SSR	SO_4 N	Moles SO_2 Absorbed/cm^2 x 10^8	N_{SO_2} x 10^6 mol/cm^2-sec	$SO_2/t_{exp}^{1/2}$ ppm/$sec^{1/2}$
34	5	0.6272	1107.9	1.0	0.02912	68.39	1.0905	6.313
35	6	0.2363	480.2	1.0	0.00278	6.54	0.2768	1.029
36	6	0.2363	480.2	1.0	0.00293	6.88	0.2912	1.029
37	6	0.4039	782.5	1.0	0.00453	10.65	0.2637	0.787
38	6	0.4039	782.5	1.0	0.00442	10.38	0.2569	0.787
39	6	0.5250	970.7	1.0	0.00621	14.59	0.2780	0.690
40	6	0.5250	970.7	1.0	0.00605	14.21	0.2707	0.690
41	6	0.6272	1107.9	1.0	0.01064	24.98	0.3983	0.631
42	6	0.6272	1107.9	1.0	0.01254	29.45	0.4695	0.631
43	7	0.6272	1107.9	1.0	0.01325	31.11	0.4961	1.894
44	7	0.6272	1107.9	1.0	0.01564	36.74	0.5858	1.894
45	7	0.5250	970.7	1.0	0.01289	30.27	0.5765	2.070
46	7	0.5250	970.7	1.0	0.01155	27.12	0.5165	2.070
47	7	0.4039	782.5	1.0	0.01124	26.39	0.6533	2.360
48	7	0.4039	782.5	1.0	0.01064	24.98	0.6185	2.360
49	7	0.2363	480.2	1.0	0.00749	17.58	0.7441	3.086
50	7	0.2363	480.2	1.0	0.00954	22.41	0.9483	3.086
51	8	0.2363	480.2	2.0	0.00239	5.62	0.2380	-0.612
52	8	0.2363	480.2	2.0	0.00286	6.71	0.2839	-0.612
53	8	0.4039	782.5	2.0	0.00769	18.06	0.4472	-0.612
54	8	0.4039	782.5	2.0	0.00589	13.84	0.3427	-0.612
55	8	0.5250	970.7	2.0	0.00749	17.58	0.3349	-0.612
56	8	0.5250	970.7	2.0	0.00769	18.06	0.3440	-0.612
57	8	0.6272	1107.9	2.0	0.00954	22.41	0.3573	-0.612
58	8	0.6272	1107.9	2.0	0.00980	23.02	0.3671	-0.612
61	9	0.5250	970.7	2.0	0.01093	25.67	0.4890	2.737
62	9	0.5250	970.7	2.0	0.01187	27.87	0.5309	2.737
63	9	0.4039	782.5	2.0	0.00980	23.02	0.5701	2.737

Table 4. Continued

No.	Case	T_{exp} sec	Re	SSR	SO_4 N	Moles SO_2 Absorbed/cm^2 x 10^8	N_{SO_2} x 10^6 mol/cm^2-sec	$SO_2/t_{exp}^{1/2}$ ppm/$sec^{1/2}$
64	9	0.4039	782.5	2.0	0.00980	23.02	0.5701	2.737
65	9	0.2363	480.2	2.0	0.00729	17.12	0.7245	2.737
66	9	0.2363	480.2	2.0	0.00811	19.06	0.8065	2.737
67	10	0.2363	480.2	2.0	0.00880	20.66	0.8744	2.359
68	10	0.2363	480.2	2.0	0.00769	18.06	0.7643	2.359
71	10	0.5250	970.7	2.0	0.01400	32.88	0.6263	2.359
72	10	0.5250	970.7	2.0	0.01325	31.11	0.5926	2.359
73	10	0.6272	1107.9	2.0	0.01480	34.75	0.5541	2.359
74	10	0.6272	1107.9	2.0	0.01564	36.74	0.5858	2.359
75	11	0.6272	1107.9	2.0	0.01654	38.84	0.6193	2.741
76	11	0.6272	1107.9	2.0	0.01701	39.94	0.6369	2.741
77	11	0.5250	970.7	2.0	0.01564	36.74	0.6998	2.741
78	11	0.5250	970.7	2.0	0.01289	30.27	0.5765	2.741
79	11	0.4039	782.5	2.0	0.01093	25.67	0.6357	2.741
80	11	0.4039	782.5	2.0	0.01064	24.98	0.6185	2.741
81	11	0.2363	480.2	2.0	0.01035	24.31	1.0288	2.741
82	11	0.2363	480.2	2.0	0.00880	20.66	0.8744	2.741
83	11	0.6272	1107.9	2.0	0.01749	41.08	0.6549	2.741
84	12	0.2363	480.2	2.0	0.00954	22.41	0.9483	2.741
85	12	0.2363	480.2	2.0	0.00929	21.81	0.9229	2.741
86	12	0.4039	782.5	2.0	0.01289	30.27	0.7494	2.741
87	12	0.4039	782.5	2.0	0.01220	28.65	0.7093	2.741
88	12	0.5250	970.7	2.0	0.01289	30.27	0.5765	2.741
89	12	0.5250	970.7	2.0	0.01654	38.84	0.7399	2.741
90	12	0.6272	1107.9	2.0	0.01701	39.94	0.6369	2.741
91	12	0.6272	1107.9	2.0	0.01564	36.74	0.5858	2.741
92	13	0.6272	1107.9	2.0	0.03084	72.44	1.1549	0.950
93	13	0.6272	1107.9	2.0	0.02997	70.39	1.1222	0.950
94	13	0.5250	970.7	2.0	0.02750	64.59	1.2302	0.950

Table 4. Continued

No.	Case	T_{exp} sec	Re	SSR	SO_4 N	Moles SO_2 Absorbed/cm^2 x 10^8	N_{SO_2} x 10^6 mol/cm^2-sec	$SO_2/t_{exp}^{1/2}$ ppm/$sec^{1/2}$
96	13	0.4039	782.5	2.0	0.02385	56.01	1.3867	0.950
97	13	0.4039	782.5	2.0	0.02318	54.44	1.3479	0.950
98	13	0.2363	480.2	2.0	0.01254	29.45	1.2461	0.950
99	13	0.2363	480.2	2.0	0.01035	24.31	1.0288	0.950
100	14	0.2363	480.2	2.5	0.00453	10.65	0.4507	1.525
101	14	0.2363	480.2	2.5	0.00430	10.11	0.4278	1.525
102	14	0.4039	782.5	2.5	0.00673	15.80	0.3913	1.525
103	14	0.4039	782.5	2.5	0.00589	13.84	0.3427	1.525
104	14	0.5250	970.7	2.5	0.00790	18.55	0.3534	1.525
105	14	0.5250	970.7	2.5	0.00769	18.06	0.3440	1.525
106	14	0.6272	1107.9	2.5	0.00749	17.58	0.2803	1.525
107	14	0.6272	1107.9	2.5	0.00769	18.06	0.2880	1.525
108	15	0.6272	1107.9	2.5	0.01654	38.84	0.6193	3.444
109	15	0.6272	1107.9	2.5	0.01564	36.74	0.5858	3.444
110	15	0.5250	970.7	2.5	0.01035	24.31	0.4631	3.444
111	15	0.5250	970.7	2.5	0.01155	27.12	0.5165	3.444
112	15	0.4039	782.5	2.5	0.00980	23.02	0.5701	3.444
113	15	0.4039	782.5	2.5	0.01007	23.66	0.5858	3.444
114	15	0.2363	480.2	2.5	0.01035	24.31	1.0288	3.444
115	15	0.2363	480.2	2.5	0.01007	23.66	1.0012	3.444
116	16	0.2363	480.2	2.5	0.01254	29.45	1.2461	5.298
117	16	0.2363	480.2	2.5	0.01254	29.45	1.2461	5.298
118	16	0.4039	782.5	2.5	0.01521	35.73	0.8847	5.298
119	16	0.4039	782.5	2.5	0.01439	33.80	0.8369	5.298
120	16	0.5250	970.7	2.5	0.01654	38.84	0.7399	5.298
121	16	0.5250	970.7	2.5	0.01701	39.94	0.7608	5.298
126	17	0.5250	970.7	2.5	0.02912	68.39	1.3027	7.947
127	17	0.5250	970.7	2.5	0.02524	59.29	1.1293	7.947
128	17	0.4039	782.5	2.5	0.02385	56.01	1.3867	7.947

Table 4. Continued

No.	Case	T_{exp} sec	Re	SSR	SO_4 N	Moles SO_2 Absorbed/cm^2	$N_{SO_2} \times 10^6$ mol/cm^2-sec	$SO_2/t_{exp}^{1/2}$ ppm/$sec^{1/2}$
129	17	0.4039	782.5	2.5	0.02129	50.01	1.2382	7.947
130	17	0.2363	480.2	2.5	0.01957	45.95	1.9447	7.947
131	17	0.2363	480.2	2.5	0.02013	47.27	2.0002	7.947
132	18	0.2363	480.2	2.5	0.02912	68.39	2.8944	15.720
133	18	0.2363	480.2	2.5	0.03461	81.29	3.4402	15.720
134	18	0.4039	782.5	2.5	0.04002	93.98	2.3268	15.720
135	18	0.4039	782.5	2.5	0.03887	91.29	2.2601	15.720
136	18	0.5250	970.7	2.5	0.04120	96.76	1.8430	15.720
137	18	0.5250	970.7	2.5	0.04002	93.98	1.7901	15.720
138	18	0.6272	1107.9	2.5	0.04368	102.57	1.6354	15.720
139	18	0.6272	1107.9	2.5	0.04120	96.76	1.5427	15.720
140	19	0.6272	1107.9	1.5	0.00790	18.55	0.2958	2.361
141	19	0.6272	1107.9	1.5	0.00880	20.66	0.3294	2.361
142	19	0.5250	970.7	1.5	0.00710	16.67	0.3175	2.361
143	19	0.5250	970.7	1.5	0.00729	17.12	0.3261	2.361
144	19	0.4039	782.5	1.5	0.00856	20.11	0.4979	2.361
145	19	0.4039	782.5	1.5	0.00530	12.46	0.3084	2.361
146	19	0.2363	480.2	1.5	0.00621	14.59	0.6176	2.361
147	19	0.2363	480.2	1.5	0.00490	11.52	0.4873	2.361
148	20	0.2363	480.2	1.5	0.01007	23.66	1.0012	5.578
149	20	0.2363	480.2	1.5	0.01220	28.65	1.2123	5.578
150	20	0.4039	782.5	1.5	0.01220	28.65	0.7093	5.578
151	20	0.4039	782.5	1.5	0.01220	28.65	0.7093	5.578
152	20	0.5250	970.7	1.5	0.01325	31.11	0.5926	5.578
153	20	0.5250	970.7	1.5	0.01439	33.80	0.6439	5.578
155	20	0.6272	1107.9	1.5	0.01325	31.11	0.4961	5.578
156	21	0.6272	1107.9	1.5	0.01289	30.27	0.4826	2.580
157	21	0.6272	1107.9	1.5	0.01289	30.27	0.4826	2.580
158	21	0.5250	970.7	1.5	0.01289	30.27	0.5765	2.580
159	21	0.5250	970.7	1.5	0.00954	22.41	0.4268	2.580

Table 4. Concluded

No.	Case	T_{exp} sec	Re	SSR	SO_4 N	Moles SO_2 Absorbed/cm^2 x 10^8	N_{SO_2} x 10^6 mol/cm^2-sec	$SO_2/t_{exp}^{1/2}$ ppm/$sec^{1/2}$
160	21	0.4039	782.5	1.5	0.00929	21.81	0.5400	2.580
161	21	0.4039	782.5	1.5	0.00904	21.23	0.5255	2.580
162	21	0.2363	480.2	1.5	0.00729	17.12	0.7245	2.580
163	21	0.2363	480.2	1.5	0.00834	19.58	0.8285	2.580
164	22	0.2363	480.2	1.5	0.01439	33.80	1.4305	7.406
165	22	0.2363	480.2	1.5	0.01400	32.88	1.3915	7.406
168	22	0.5250	970.7	1.5	0.01654	38.84	0.7399	7.406
169	22	0.5250	970.7	1.5	0.01701	39.94	0.7608	7.406
170	22	0.6272	1107.9	1.5	0.01654	38.84	0.6193	7.406
171	22	0.6272	1107.9	1.5	0.01701	39.94	0.6369	7.406
172	23	0.6272	1107.9	1.5	0.01799	42.24	0.6735	6.119
173	23	0.6272	1107.9	1.5	0.01749	41.08	0.6549	6.119
174	23	0.5250	970.7	1.5	0.01521	35.73	0.6806	6.119
175	23	0.5250	970.7	1.5	0.01799	42.24	0.8046	6.119
176	23	0.4039	782.5	1.5	0.01480	34.75	0.8605	6.119
177	23	0.4039	782.5	1.5	0.01439	33.80	0.8369	6.119
179	23	0.2363	480.2	1.5	0.01362	31.98	1.3535	6.119

APPENDIX D

PHYSICAL PARAMETERS

Table 5. Physical Parameters

	Units	Value
DROP RATE	drops/sec	2.86
WATER FLOW RATE	cm^3/min	2.01
DROP VOLUME	cm^3	0.0117
DROP DIAMETER	cm	0.282
DROP AREA	cm^2	0.250
DROP DENSITY	g/cm^3	0.9999
DROP VISCOSITY	g/cm-sec	0.0143
DROP TEMPERATURE	°C	8.
VAPOR PRESSURE	mm Hg	8.05
DROP MOLECULAR WEIGHT	g/gmol	18.0
GAS DENSITY	g/cm^3	0.00125
GAS VISCOSITY	g/cm-sec	0.000165
GAS MOLECULAR WEIGHT	g/gmol	28.
DIFFUSIVITY OF H_2O IN N_2	cm^2/sec	0.22
GAS FLOW RATE	liters/min	3.6

BIBLIOGRAPHY

1. T. Akiyama, "The Equivalence of the Penetration and Boundary Layer Theories," Chem. Eng. Sci., 27, 161 (1972).

2. J. B. Angelo, E. N. Lightfoot, and D. W. Howard, "Generalization of the Penetration Theory for Surface Stretch: Application to Forming Oscillating Drops," J. Am. Inst. Chem. Engr., 12(4), 751 (1966).

3. G. P. Arklipova, K. P. Mishchenko, and I. E. Flis, "Equilibrium in Dissolution of Gaseous SO_3 in Water at 10-35°C," Zh. Prik. Khim., 41(5), 1131 (1968).

4. W. J. Beek and H. Kramers, "Mass Transfer with a Change in Interfacial Area," Chem. Eng. Sci., 16, 909 (1962).

5. C. O. Bennett and J. E. Myers, Momentum, Heat and Mass Transfer, Second Edition, McGraw-Hill Book Co., New York, 1974.

6. R. B. Bird, W. E. Stewart, and E. N. Lightfoot, Transport Phenomena, John Wiley and Sons, Inc., New York, 1960.

7. O. A. Bagaevskii, "Adsorption of a Gas on a Growing Drop," Zh. Fiz. Khim., 43, 1298 (1969).

8. H. S. Carslaw and J. C. Jaeger, Conduction of Heat in Solids, Claredon Press, Oxford, 1947.

9. J. M. Coulson and S. S. Skinner, "The Mechanism of Liquid-Liquid Extraction Across Stationary and Moving Interfaces--I. Mass Transfer Into Single Dispersed Drops," Chem. Eng. Sci., 1(5), 197 (1952).

10. J. Crank, The Mathematics of Diffusion, Claredon Press, Oxford, 1956.

11. P. V. Danckwerts, Gas-Liquid Reactions, McGraw-Hill Book Co., New York, 1970.

12. P. V. Danckwerts, "Significance of Liquid-Film Coefficients in Gas Absorption," Ind. Eng. Chem., 43(6), 1460 (1951).

13. J. T. Davies and E. K. Rideal, Interfacial Phenomena, Second Edition, Academic Press, New York, 1963.

BIBLIOGRAPHY (Continued)

14. J. L. Davis, "Absorption of SO_2 by Charged Aqueous Droplets," M.S. Thesis, Georgia Institute of Technology (1972).

15. B. E. Dixon and A. A. W. Russell, "The Absorption of CO_2 by Liquid Drops," J. Soc. Chem. Ind., 69, 284 (1950).

16. W. Drost-Hansen, "Molecular Aspects of Aqueous Interfacial Structures," J. Geophys. Res., 77(27), 5132 (1972).

17. T. E. Eriksen, "Diffusion Studies in Aqueous Solutions of SO_2," Chem. Eng. Sci., 24, 273 (1964).

18. Frank-Kamenetskii, Diffusion and Heat Exchange in Chemical Kinetics, Princeton Univ. Press, Princeton, N. J., 1955.

19. N. A. Fuks, Evaporation and Droplet Growth in Gaseous Media, Pergamon Press, New York, 1959.

20. F. H. Garner, A. Foord, and M. Tayeban, "Mass Transfer from Circulating Liquid Drops," J. Appl. Chem., 9, 315 (1959).

21. F. H. Garner and A. H. P. Skelland, "Mechanism of Solute Transfer from Droplets," Ind. Eng. Chem., 461, 1255 (1954).

22. P. J. Giardina, "The Effects of Humidity and Gas Phase Concentration on the Absorption of SO_2 by Charged Aqueous Droplets," M.S. Thesis, Georgia Institute of Technology (1973).

23. P. M. Griffith, "Mass Transfer from Drops and Bubbles," Chem. Eng. Sci., 12, 198 (1960).

24. H. Groothius and H. Kramers, "Gas Absorption by Single Drops During Formation," Chem. Eng. Sci., 4, 17 (1955).

25. P. M. Heertjes, W. A. Holve, and H. Talsma, "Mass Transfer Between Isobutanol and Water in a Spray Column," Chem. Eng. Sci., 3, 78 (1954).

26. P. M. Heertjes and L. H. Denie, "The Mechanism of Mass Transfer During Formation, Release and Coalescence of Drops--II. Quantitative Predictions, Coalescence and Release," Chem. Eng. Sci., 26, 697 (1971).

27. G. M. Hidy and J. R. Brock, The Dynamics of Aerocolloidal Systems, Pergamon Press, New York, 1971.

28. R. Higbie, "The Rate of Absorption of a Pure Gas Into a Still Liquid During Short Periods of Exposure," Trans. Am. Inst. Chem. Engr., 31, 365 (1935).

BIBLIOGRAPHY (Continued)

29. P. R. Hughes and E. R. Gilliland, "Mass Transfer Inside Drops in a Gas," Chem. Eng. Prog. Symp. Series, 51(16), 101 (1955).

30. A. I. Johnson and A. E. Hamielec, "Mass Transfer Inside Drops," J. Am. Inst. Chem. Engr., 6(1), 145 (1960).

31. H. F. Johnstone and P. W. Leppla, "The Solubility of SO_2 at Low Partial Pressures. The Ionization Constant and Heat of Ionization of Sulfurous Acid," J. Am. Chem. Soc., 56, 2233 (1934).

32. G. Jones and W. H. Ray, "The Surface Tension of Solutions of Electrolytes as a Function of the Concentration. A Differential Method for Measuring Relative Surface Tension," J. Am. Chem. Soc., 59, 187 (1937).

33. C. J. King, "The Additivity of Individual Phase Resistances in Mass Transfer Operations," J. Am. Inst. Chem. Engr., 10(5), 671 (1964).

34. V. G. Levich, Physiochemical Hydrodynamics, Prentice-Hall, Inc., Englewood Cliffs, N. J., 1962.

35. W. Licht and J. B. Conway, "Mechanism of Solute Transfer in Spray Towers," Ind. Eng. Chem., 42(6), 1151 (1950).

36. W. Licht and W. F. Pansing, "Solute Transfer from Single Drops in Liquid-Liquid Extraction," Ind. Eng. Chem., 45(9), 1885 (1953).

37. P. S. Liss, "Exchange of SO_2 Between the Atmosphere and Natural Waters," Nature, 233, 327 (1971).

38. S. Lynn, J. R. Straatemeier, and H. Kramers, "Absorption Studies in the Light of the Penetration Theory--III. Absorption by Wetted Spheres, Singly and in Columns," Chem. Eng. Sci., 4(2), 63 (1955).

39. D. MacLeod and B. Ermit, "Absorption of Oxygen by Water Drops," Effl. Wat. Treat. J., 12, 407 (1972).

40. M. J. Matteson and P. J. Giardina, "Mass Transfer of SO_2 to Growing Droplets, Role of Surface Electrical Properties," Env. Sci. Tech., 8, 50 (1974).

41. J. H. Perry, Ed., Chemical Engineers' Handbook, Third Edition, McGraw-Hill Book Co., New York, 1950.

42. A. T. Popovich, R. F. Jarvis, and O. Trass, "Mass Transfer During Single Drop Formation," Chem. Eng. Sci., 19, 357 (1964).

BIBLIOGRAPHY (Continued)

43. A. T. Popovich and J. Lenges, "Experimental Study of Mass Transfer During Single Drop Formation, Release and Fall," Thermo. Fluid Dyn., 4(2), 87 (1971).

44. J. M. Prausnitz, Molecular Thermodynamics of Fluid-Phase Equilibria, Prentice-Hall, Inc., Englewood Cliffs, N. J., 1969.

45. S. M. Rajan and W. J. Heideger, "Drop Formation Mass Transfer," J. Am. Inst. Chem. Engr., 17(1), 202 (1971).

46. V. M. Ramm, Absorption of Gases, Israel Program for Scientific Translation, Jerusalem, 1968.

47. P. M. Rose and R. C. Kintner, "Mass Transfer from Large Oscillating Drops," J. Am. Inst. Chem. Engr., 12(3), 530 (1966).

48. E. Ruckenstein, "A Generalized Penetration Theory for Unsteady Convective Mass Transfer," Chem. Eng. Sci., 23, 363 (1968).

49. L. C. Schroeter, Sulfur Dioxide, Pergamon Press, New York, 1966.

50. R. W. Schrage, A Theoretical Study of Interphase Mass Transfer, Columbia University Press, New York, 1953.

51. T. K. Sherwood, J. E. Evans, and J. V. A. Langcor, "Extraction in Spray and Packed Columns," Trans. Am. Inst. Chem. Engr., 35, 597 (1939).

52. T. K. Sherwood and R. L. Pigford, Absorption and Extraction, McGraw-Hill Book Co., New York, 1952.

53. A. H. P. Skelland and R. M. Wellek, "Resistance to Mass Transfer Inside Drops," J. Am. Inst. Chem. Engr., 10(4), 491 (1964).

54. F. P. Terraglio and R. M. Manganelli, "The Absorption of Atmospheric SO_2 by Water Solutions," J. Air Poll. Cont. Assn., 17(6), 403 (1967).

55. R. E. Treybal, Mass Transfer Operations, Second Edition, McGraw-Hill Book Co., New York, 1955.

56. F. H. H. Valentin, Absorption in Gas-Liquid Dispersions, E. & F. N. Spon, Ltd., London, 1967.

57. H. C. Ward, Personal Communication, Georgia Institute of Technology (1974).

BIBLIOGRAPHY (Concluded)

58. R. C. Weast, Editor, Handbook of Chemistry and Physics, 47th Edition, Chemical Rubber Co., Cleveland, 1966.